MIL-HDBK-733
27 JUNE 1986

MILITARY STANDARDIZATION HANDBOOK

NONDESTRUCTIVE TESTING METHODS OF COMPOSITE MATERIALS - RADIOGRAPHY

NO DELIVERABLE DATA REQUIRED BY THIS DOCUMENT

AREA NDTI

AMSC N/A

Approved for public release; distribution unlimited.

DEPARTMENT OF DEFENSE
WASHINGTON, D.C. 20301

MIL-HDBK-733
MILITARY HANDBOOK FOR NONDESTRUCTIVE TESTING
METHODS OF COMPOSITE MATERIALS - RADIOGRAPHY

1. This standardization handbook was developed by the Department of Defense with the assistance of the Army Materials Technology Laboratory, and Dr. Frank P. Alberti of the University of Lowell, Lowell, Massachusetts, in accordance with established procedure. It is approved for use by all Department and Agencies of the Department of Defense.

2. It is the intent to review this handbook periodically to insure its completeness and currency. Users of this document are encouraged to report any errors discovered and any recommendations for changes or inclusions to Army Materials Technology Laboratory, ATTN: SLCMT-MSR-ES, Arsenal Street, Watertown, MA 02172-2719.

FOREWORD

1. This handbook will eventually become a chapter in a larger volume which will probably include the following chapters:

Radiography, A State-of-The-Art-Review
Ultrasonics, A State-of-The-Art-Review
Acoustic Emission, A State-of-The-Art-Review
Thermography, A State-of-The-Art-Review

2. Each chapter will be coordinated separately as the amount of materials to review at one time is large. After acceptance of the individual chapters as smaller handbooks, they will be incorporated into a single volume.

3. It is intended that this volume serve as a reference in which answers may be found to the more general questions concerning the technical aspects and applications of radiography to composites.

TABLE OF CONTENTS (Continued)

TABLE OF CONTENTS (Continued)

TABLE OF CONTENTS (Continued)

1.0 SCOPE

1.1 General This document is intended to provide information on radiographic techniques for examining discontinuities found in many types of reinforced composites. The handbook contains varied information from the detection of discontinuities by enhancement methods to the various techniques used such as microradiography, stereoradiography and neutron radiography. The fundamentals of radiography are not included as this type of information is available in MIL-HDBK-728/5.

2.0 REFERENCED DOCUMENTS

2.1 Government documents.

2.1.1 Specifications, standards, and handbooks. Unless otherwise specified, the following specifications, standards, and handbooks of the issue listed in the issue of the Department of Defense Index of Specifications and Standards (DoDISS) specified in the solicitation form a part of this standard to the extent specified herein.

Handbook

MIL-HDBK-728 Nondestructive Testing

2.2 Other publications. The following documents form a part of this standard to the extent specified herein. The issues of the documents which are indicated as DoD adopted shall be the issue listed in the issue of the DoDISS specified in the solicitation. The issues of documents which have not been adopted shall be those in effect on the date of the cited DoDISS.

2.2.1 Technical articles referenced in this handbook are listed at the end of this handbook.

(Nongovernment standards are generally available for reference from libraries. They are also distributed among technical groups and using Federal agencies.)

3.0 DEFINITIONS

None.

4.0 COMPOSITE MATERIAL INVESTIGATIONS

4.1 Introduction. This handbook is the compilation of the experiences of many research persons. References included in the handbook are cited so that the individual can obtain more specific information on the particular subject of interest. The handbook will be updated as more users contribute their works.

4.2 Effect of scattered radiation on composites. In the radiography of composites, which are comprised of low and medium density materials, scattered radiation forms a high percentage of the total radiation reaching the film. This is due to the nature of the soft, low voltage radiation used to radiograph these materials, which is inherently less penetrating and more subject to scatter. However, if higher, more penetrating voltages were used, excessive overall film density could occur, resulting in reduced contrast and a radiograph unreadable in terms of flaw detection. Scatter is, therefore, a major problem when radiographing composites. In general this presents a paradox for the radiographer since low voltages are desirable for improving subject contrast, but lead to fogging of the image due to scatter, which, in turn, reduces subject contrast.

4.3 Penetrameters for composite materials. Concerning the use of penetrameters to measure the sensitivity of a composite material radiographic investigation, the question, of what type of penetrameter design or material should be used is difficult to answer; at this time, specifications are non-existent for adequate penetrameter measurement requirements for composite materials. There are a number of possible approaches to this problem. Penetrameters similar in design to those presently used could be made from a material representative of the particular composite specimen. However, at best this would yield only a rough measurement, because of the complex composition of most composite materials. In addition, the design of an adequate penetrameter is very difficult because of the many types of imperfections associated with composite specimens (fiber misalignment, fiber breaks, resin content irregularities, fiber matrix unbonds, damage considerations, moisture effects, etc.).

4.4 Other penetrameter approaches. Another approach might be to incorporate simulated defects into the penetrameter. For example, in the inspection of a fiber-reinforced composite, a single ply of defective composite could be used as a comparative quality standard when radiographed together with the specimen. In any case, the selection of a penetrameter range for which a radiograph may be properly read is also specified in reference to penetrameters. One penetrameter can be used for each area of the specimen where the density of the radiographic image does not vary more than + 30% or - 15% from the density of the image of the penetrameter. To cover an entire radiograph of widely divergent density, two penetrameters must be used, one placed at the highest density region and the other at the lowest. This requirement was included in the specifications in order to control the density of radiographs, since density plays such an important part in sensitivity, contrast and defect detection ability.

4.5 Types of defects. By far the most widely used radiographic technique for the inspection of composite materials is the straightforward radiographic method. It has been shown that the density on a radiograph depends upon the relative absorption of radiation by the material or defects in its path. In composite material investigations, the radiographer has had to deal with a vast spectrum of reinforcement and matrix material systems, together with a

number of associated types of defects. In particular, some of the defect considerations investigated with radiography include: bond evaluations, curing effects, damage considerations, flaw content and growth, voids, failure mechanisms, fatigue behavior, fiber characteristics and fiber breaks, fracture characteristics, moisture effects, physical properties, resin content, and thermal effects. The need for detection of these types of defects and the general nature of composite systems has brought about a number of advancements in the traditional, straightforward radiographic technique, and has spurred the development of some new and promising techniques.

4.6 Sampling for an early study. In an early composite investigation, Owston and Connor[1] reported the initial results of an extended research program to determine the defects which initiate mechanical failure in carbon fiber-reinforced plastics, and to find nondestructive evaluation (NDE) methods of locating these defects. Approximately 40 specimens, some short rectangular bars, others cylindrical rings, were investigated. The rectangular bars were 1.5 in. x 0.75 in. x 0.08 in. thick, unidirectional with fibers running lengthwise, and were made by stacking carbon fiber-epoxy prepreg tapes. The cylindrical rings were 4.25-in. inside diameter by 0.1-in. wall thickness, and were an attempt to produce a tensile stress in unidirectional material without the complication of grips.

4.6.1 Operating parameters. Good quality radiographs were obtained at 12 kV using a beryllium window x-ray tube, Kodak Microtex double-sided industrial film, and a source-to-film distance of 24 inches. Black industrial polyethylene was used as a film cassette in some cases, while other exposures were made without a cassette but with all the equipment enclosed in a dark room. Similar results were achieved in both cases. For the ring specimen, a strip of film backed with a thick strip of lead was fitted inside the ring, and the entire assembly was rotated in front of a collimated beam from the x-ray generator. The resulting radiographs revealed porosity in the specimens, but could not resolve the fibers, their orientation, or density.

4.6.2 Classification of composite defects. Composite defects are classified into three groups, Type 1, Type 2 and Type 3.

4.6.2.1 Type 1 defects. Type 1 defects: Those of large proportions affecting wide areas or even the whole of a component, e.g., omission of a layer of prepreg in the layup of a component, faulty resin curing, incorrect compaction due to failure to close the mold correctly.

4.6.2.2 Type 2 defects. Type 2 defects: Smaller scale defects which are still the result of manufacturing technique, e.g., voidage, local misorientation of fibers, local variations in resin content, shrinkage cracks in the resin, and unavoidable features in the structure such as joints in prepreg sheets.

4.6.2.3 Type 3 defects. Type 3 defects: Very small defects, e.g., single misoriented fibers and their associated entrained air bubbles, piping along single fibers. These defects are the ultimate defects, the ones that cannot be avoided except under exceptionally rigorous manufacturing conditions.

4.6.3 Detection of discontinuities. The larger voids and cracks associated with type 2 are readily detectable radiographically. Experience with the failure of test specimens has led Owston and Connor to believe that much attention should be paid to the significance of these defects. In some

specimens containing large Type 2 defects, failure initiated at apparently insignificant Type 3 defects, implying that defect form and location can be very important.

4.6.3.1 Detection of fiber fraction and orientation. Variations in fiber fraction and orientation do not appear to be readily detectable using radiography or ultrasonics, although some indications can be obtained radiographically by using glass fiber tracers (a form of image enhancement).

4.7 Fiber failure of boron-epoxy laminates. In a more recent study, Roderick and Whitcomb[2] describe how a modified x-ray method can be used to show how fibers fail during fatigue of boron-epoxy laminates. The authors employed x-radiography in tracking fiber breakage in two notched boron-epoxy laminates, (+45/0/-45/0) and (90/±45/0) that were subjected to constant amplitude cyclic loads. Prior to the fatigue test, broken fibers were found only very close to the notch (as a result of machining). After 10^6 applied load cycles, a number of additional fibers were broken, as evidenced on the radiographs. At 5×10^6 applied load cycles, more fiber breaks were recorded.

4.7.1 Technique. In this modified x-ray method, a high resolution glass photographic plate was used to record the image of the 1-mm thick specimens. The x-ray source was 12 inches from the laminate, which was laid on the photographic plate. The exposure was 5 minutes at 50 kV and 20 mA. After the plate was developed, it was rephotographed with a metallograph to produce a magnified image. The authors suggest that this technique can be used to locate fiber breaks on the glass plates themselves, and that the significance of this technique can be seen by noting the similarity between the images obtained in this study with thermographs of the same laminates at various stages of loading.

4.8 Identification of fiber breakage and matrix cracking. Roderick and Whitcomb[3] employed a similar technique to identify the primary fatigue mechanisms and to study the sequency of events during fatigue failure of notched boron-epoxy laminates. X-radiography and scanning electron microscopy were used in combination to examine the fatigue processes in notched (0, ±45. 90) laminates. Fiber breakage and matrix cracking were monitored. Fiber breakage was detected by taking radiographs at no load and periodically during fatigue testing. Soft, 50-kV radiation at 20 mA and a source-to-film distance of 30 cm were used to expose high resolution photographic glass plates which were processed and examined on a metallograph at 50X magnification. The breaks in the tungsten core of the boron fibers could easily be seen.

4.8.1 Examination of fiber damage. Examinations of each series of radiographs revealed that, initially, fatigue damage in both the (0, ± 45.90) laminates occurred as interlaminar cracks around the edge of a notched hole. Then, whenever further damage developed, interlaminar cracks in the ± 45-degree plies began to propagate from the edge of the hole. Finally, in both type laminates, primarily ± 45-degree fibers broke (prior to two-piece failure) where interlaminar cracks in the ± 45-degree plies had occurred. The results of this study suggest that in boron-epoxy laminates, the 45 degree plies play a key role in the fatigue process, since fatigue starts as interlaminar matrix cracks in the ± 45-degree plies. Radiography has thus been shown to be a valuable investigative tool in the study of composite fatigue behavior.

4.9 Performance of various classes of resin in carbon fiber composites. In another investigation, Artis and Joiner[4] employed a stereo-micro-radiography technique together with a molten sulfur impregnation to measure the relative performance of various classes of resin in carbon fiber composites. Unidirectional carbon-fiber-reinforced plates were fabricated with each of seven different resins, including: EPIKOTE 828 (epoxy), ARALDITE MY 753/HY 951 (epoxy), CRYSTIC 199 LV (polyester), CRYSTIC 272 and 625 LV (polyester), DV 19162 VARNISH (phenolic) and QX 13 Resin (polyimide). The plates fabricated were 7.62 cm x 7.62 cm x 0.2 cm thick, and were cut into 1.0 cm wide strips perpendicular to the fiber direction.

4.9.1 Enhancement of small voids. In order to enhance the radiographic image of very small voids (with diameters of five microns or less), a method of electron staining was developed. It was postulated that if the micropores of the carbon composite could be completely filled with a "staining" liquid having a sufficiently higher electron density than carbon, and furthermore, if the liquid could be kept from evaporating during radiography, then the pore network would predominate in the radiograph over the matrix. Molten sulphur was found to be an excellent medium, wetting all types of consolidated carbons, and was applied to the samples (after fine surface grinding), using a simple vacuum impregnation technique.

4.9.2 Examination of channel network pores. The samples were radiographed at 12 kV for 30 seconds with a source-to-film distance of 25.4 cm at an offset angle of 11° 18", while they were placed in contact with the film and exposed in a light tight box. The radiographs were then enlarged using a microscopic technique, and stereo pairs were assembled by contact printing the films on Ilford 11/0 paper. This method of radiography proved particularly advantageous in that it allowed the examination of channel network pores within the specimen and not surface pores alone.

4.9.3 Results. The stereo pairs produced showed voids in all the samples; however, the epoxy resins showed the least void occurrence. The voids in the polyester resin occurred along the fibers, the most probable source being air that was allowed to enter the composite due to the resin's low fiber wetting ability. Both phenolic and polyimide resins showed similar voids. The polyimide radiographs showed particularly bad striation, thought to be due to resin starvation.

4.9.4 Conclusions. From their findings, the authors concluded that epoxy resins permit less void formation than the other resins, due to the epoxy resin's better wetting ability. They also concluded that the technique of stereo-microradiography could be extremely useful in the evaluation of carbon fiber composite materials, and that attempts should be made to devise a simple method of numerically quantifying the image produced.

4.10 Microradiography.

4.10.1 General. In order to improve image detail quality and radiographic sensitivity, a special radiographic method and related equipment were devised which best utilize the beneficial effects of very small focal spot size and improved, low kV subject contrast. This technique, microradiography, employs soft radiation in the 5-to 50-kV range, generated by special x-ray tubes with very small focal spots. The specimen must be kept in intimate contact with the film to minimize any geometrical enlargement effects. This is accomplished

either by simple clamping devices or by using a vacuum pressure device. The film used is usually coated on one side only with a very fine grained emulsion (finer than that of typical x-ray films).

4.10.2 Technique. The microradiography technique is particularly suited to obtaining images of thin specimens of low density; for this reason, it is being used more and more extensively for composite material investigations. The detail and radiographic quality obtained with a successful application of this technique can be extremely good. However, there are some difficulties which must be considered when employing a low energy x-ray method such as this. One difficulty, depending upon the thickness of the specimen and the source-to-film distance used, is that exposure times can be very long, three hours or more. This exposure time could be reduced by decreasing the source-to-film distance to a minimum (which is an advantage of having a very small focal spot), but the specimen area intercepted by the radiation beam would also be reduced. Also, in the low kilovoltage range (20 kV or below), the inverse square law normally governing radiation intensity is violated due to the absorption of these low energy x-rays by the air. Moreover, the film cassette material also plays a part in radiation absorption and should be of minimum thickness and density. Many radiographers use plastic or paper film holders reinforced with tape and a thin lead back screen (0.005 or 0.01 inch thick). The paper holder should be of fine grained paper since radiation in the 20-50 kV range will transfer the holder paper grain image onto the film. The holders should also be free from dust, pencil, or paint smudges that would also be revealed on the radiograph and could be incorrectly interpreted as material defects. An extended daily warm-up period is required for microradiographic tubes which are highly susceptible to sudden voltage surges and usually require that a voltage regulator be installed in the line. In addition, care must be taken not to touch or jar the x-ray tube; because of its small focal spot size, even a slight movement can cause significant misorientation of the radiation beam. Beam misalignment can cause considerable blurring, particularly for investigations of specimens containing slots. Finally, since the objects radiographed are usually thin, the defect features to be detected are usually quite small and require some type of enlargement for adequate viewing and interpretation.

4.10.3 Effects of low voltage radiation. These difficulties and others were discussed by Huggins[5] who related the results of his recent investigations with low energy radiation. Huggins relates that at x-ray energies below about 60 kV, we begin to be concerned with the absorption of materials between the x-ray source and the film, other than the object being radiographed. As x-ray energy is reduced, this absorption has two unwanted effects; it reduces the intensity of the beam thus increasing exposure time, and it preferentially absorbs the low energy components of the spectrum thus reducing radiographic contrast. For these reasons, use of plastic rather than aluminum-fronted cassettes is necessary with x-ray energies below about 40 kV. At around 16 kV, the granular structure of the plastic window begins to be apparent.

4.10.4 Effects of x-ray tube window. The material of the x-ray tube window has an increasingly marked effect on x-ray transmission below about 50 kV. Thus, if radiation of much less energy is required, the tube will need to have a low absorptive window. This will usually be of beryllium and have a thickness of less than 2 mm. A 1-mm window gives good transmission down to about 6 kV.

4.10.5 Radiation attenuation below 20 kV. Radiation attenuation due to the air between the film cassette and the x-ray tube window begins to be significant below about 20 kV, depending on the focus-to-film distance used. The problem can be dealt with by using either a low density gas environment, such as hydrogen or helium, or by radiographing in a vacuum. Huggins used helium because it is safer than hydrogen, and its x-ray transmission is only marginally less. For example, with 4 kV x-rays, 200 mm of helium has a transmission of 99.6%. The corresponding transmission of air is 17%. Use of a vacuum, Huggins reports, could result in increased x-ray absorption, since the inlet and exit windows would need to be strong enough to support atmospheric pressure; helium on the other hand, can be contained in a vessel with extremely thin Mylar windows at either end. Huggins goes on to discuss various forms of enlargement techniques and the effects of film type and magnification, as well as the use of photographic plates on enlarged image detail and quality.

4.10.6 Measurement of fatigue damage in boron-epoxy composite laminates. In an investigation similar to that of Roderick and Whitcomb, [2, 3] Marcus and Stinchcomb [6] measured fatigue damage in boron-epoxy composite laminates using a microradiography technique. From previous investigations, it was evident to the authors that two different effects must be considered in order to understand the mechanical behavior (static and cyclic) of composite laminates with a stress raiser such as a circular hole. These effects are (1) the increased stress near the hole due to the local stress raiser effect, and (2) the interlaminar stresses occurring at and near the hole due to the presence of the free edge. See Figures 1-4 (given as Figures 3, 4, 5 and 6 in Ref. 6).

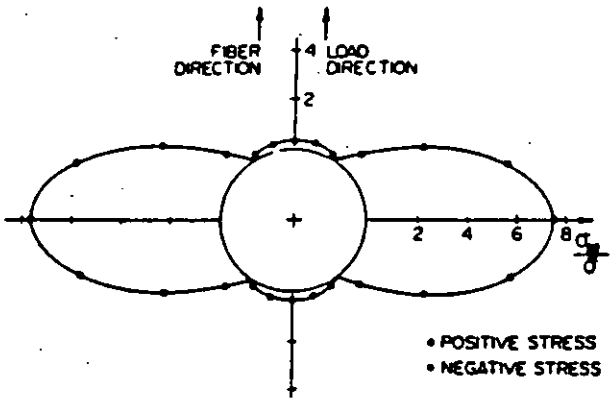

FIGURE 1. Circumferential normal stresses in 0-degree layers (z =h/2 and 7h/2).[6]

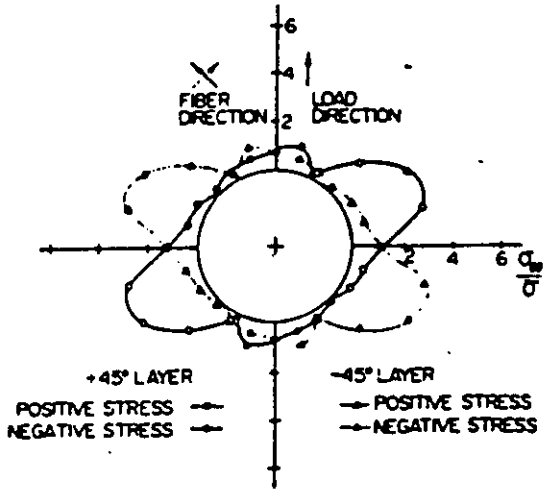

FIGURE 2. Circumferential normal stresses in 45-degree layers (z=7h/4 and 9h/4).[6]

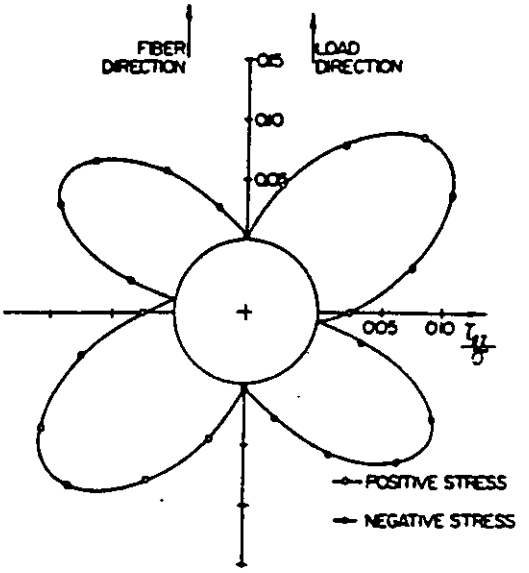

FIGURE 3. Interlaminar shear stresses in top 0-degree layer (z = 7h/2).[6]

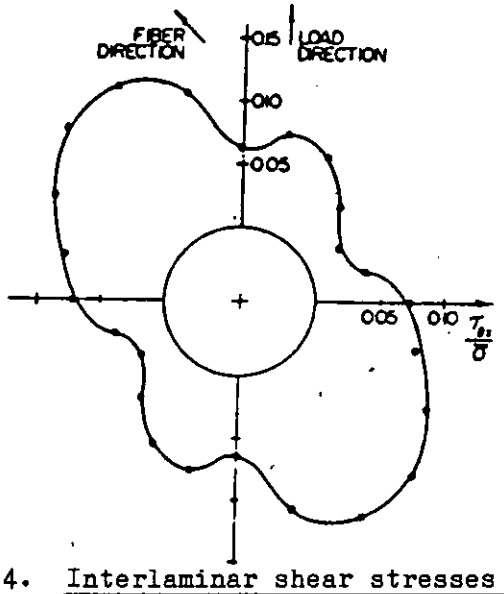

FIGURE 4. Interlaminar shear stresses in +45-degree layer (z = 9h/4).[6]

4.10.6.1 Type of analysis. In this investigation, a three-dimensional finite-element analysis was used to predict the static-stress distribution around a circular hole in a (0/±45/0) boron-epoxy plate. Data, obtained by the thermographic and radiograpic techniques during cyclic-strain tests on similar specimens, revealed the contribution of the two above-mentioned effects on the fatigue behavior of the composites. The tests performed were a series of strain-controlled tension-tension fatigue tests on a 0.05-inch (0/±45/0) specimen layed-up from AVCO 5505 prepreg tape.

4.10.6.2 Operating parameters. For the radiographic investigation, a point x-ray source with a nickel filter, operating at 25 kV and 10 mA, produced radiation which was collimated by an 18-in. long by 7/8-in diameter lead-shrouded tube. The thin specimen to be radiographed was placed between the end of the tube and a sheet of Polaroid Type 57 film. The exposure time was 25 seconds.

4.10.6.3 Relationship between damaged areas and intense heat. A sequence of radiographs of the specimen, corresponding to a similar series of thermographic images, was made by stopping the test at various points and performing the radiography. The comparisons showed that the more heavily damaged regions are also regions of more intense heat development.

4.10.6.4 Development of damage. The process by which the damage develops, as shown in the radiographs and by visual observation of the specimen during testing, is one in which the 0-degree layer longitudinal crack in the matrix develops first, followed by ejection of short pieces of the broken 45-degree fibers as the longitudinal crack propagates through the thickness and by delamination between the 45-degree layers. The authors noted that damage developed quickly in the material and then, for all purposes, stopped as could be seen by comparing the radiographs.

4.10.6.5 Analysis of effects of the stress state on fatigue behavior. From the theoretical stress state around the hole and experimentally observed fatigue behavior noted, an analysis of the effects of the stress state on the fatigue behavior was made. The authors reported that the result of this investigation implied that a crack, although it initiates at points of greatest strain-energy density in the outer 0-degree layer, initiates preferentially in quadrants II and IV under the influence of the interlaminar shear stress in the underlying +45-degree layer. One must deduce this mechanism, suggest the authors, from a consideration of the stress state at the hole boundary.

4.10.7 Benefits of contact microradiography over microphotography. In another investigation, Darlington and McGingley[7] discussed the benefits of contact microradiography over microphotography for determining fiber orientation and distribution in short fiber-reinforced plastics. The contact microradiography (CMR) technique consists of making a microradiograph of a 100-micron slice of the composite. This was compared to a microphotograph made on a polished microtomed section of a 100-micron slice of the same specimen. The microradiograph showed not only the parts of the fibers penetrating the polished surface, but also those underneath the surface to a depth of 100 microns. Therefore, a single circular spot indicated good fiber alignment along the axis, while blurred strip-like areas indicated that fibers were misaligned with the axis. Examples shown indicated gross misalignment at section corners and adjacent to complex shapes.

4.10.7.1 Estimation of orientation of fibers to plane of the cut. The use of a slice whose thickness was less than the mean fiber length suggested to the authors the possibility of estimating, from the radiograph, the orientation of the fibers to the plane of the cut. Therefore, the authors contended, one slice cut perpendicular to the molded surface can give a good indication of the quality of the molding process by showing a 3-dimensional orientation distribution through the thickness. Also, the examination of a number of such cuts or a variety of cuts made at selected angles could be used for a more complete examination.

4.11 Automatic computer-based radiographic image enhancement.

4.11.1 General. While visual inspection and interpretation continues to be the most widely used technique for defect detection, the increasing need for more rapid and more accurate acceptance/rejection decisions has spurred the development of automatic, computer-based image enhancement and analysis systems. Over the past few years, a number of systems have been developed, some of which provide various forms of image enhancement, and others which provide both enhancement and image analysis.

4.11.2 Electronic enhancement. In one of the earlier papers [8] on radiographic image enhancement, Vary states that, since the usual methods of direct or optically aided viewing require a high degree of eye accommodation, there is a growing effort to increase the amount of information retrievable from radiographs by means of image enhancement techniques. In this early report, radiographs of nuclear and aerospace components were studied with a closed-circuit television system to determine the advantages of electronic enhancement. The radiographic images were examined on a television monitor under various degrees of magnification and enhancement. The enhancement was accomplished by generating a video signal whose amplitude was proportional to the rate of change of image density. Points, lines, edges, and other density variations that were faintly registered in the original image were thus rendered in sharp relief.

4.11.2.1 Electronic enhancement vs optical examination. With some exceptions, neither the normal nor enhanced video displays revealed details of the radiographs that could not be ultimately seen by direct-eye viewing or by means of simple optical aids. With proper back-lighting, magnification, and eye accommodation, Vary states, there is actually little information in well-made radiographs that escapes detection. Conversely, the video system does retrieve all details revealed by close optical examination. However, all these details could not always be retrieved simultaneously with one setting of the enhancement controls (of this particular system), because the density response range of the system was not always adequate.

4.11.2.2 Identification of artifacts. One problem that was aggravated by edge enhancement arose from film artifacts, such as the presence of defects in the film emulsion, graininess, scratches, water marks, dust, lint, etc. All these were, of course, enhanced along with other image details. In most instances, such artifacts that appeared in the enhancement could be readily identified and ignored, as in conventional radiographic examinations, after a little experience was gained in interpreting the enhanced images.

4.11.2.3 Value of video system. Overall, the video system proved to be a valuable tool for the examination of radiographs. Over 100 samples of radiographs were examined and interpreted with the aid of the enhancer. Each was found to contain some detail that was either missed or difficult to see without enhancement.

4.11.3 Further study in flaw detection. In a more recent report, Jacoby[9] described his ongoing investigations in the use of automatic computer-based signal processing techniques for image enhancement of radiographs of aerospace composite structures. He begins by pointing out that improvement of the visual image does not mean finding increasingly small flaws

more reliably, but that an NDT technique should detect all the flaws that would adversly influence the performance of the composite structure. "The problem", Jacoby explained, "is due less to the NDT techniques themselves than to the current dependency on subjective evaluations of data by inspectors". The lack of consistency in the interpretation of x-ray images has been called "the weakest link" in the whole inspection process.

4.11.3.1 Improvement in interpretation and evaluation of data. Automatic computer-based signal processing techniques improved the interpretation and evaluation of NDT data in two important ways. First, the data was enhanced to accentuate details which would otherwise not be apparent to the observer and second, the enhanced data was automatically evaluated by the computer, and the item was accepted or rejected on the basis of a predetermined defect size criterion without relying exclusively on the subjective interpretation of an inspector.

4.11.3.2 Signal processing techniques. The paper described how several new and innovative signal processing techniques for image data enhancement and restoration have been combined to provide an automatic computer-based method for measuring voids on radiographs of graphite/epoxy composite structures. The techniques employed included high-pass filtering, low-pass filtering (smoothing), thresholding, requantization, and contrast stretching to produce a binary image from a radiograph. Then the computer -- in this case a Data General Eclipse 130--evaluation the binary image, counted voids, measured them, and either accepted or rejected the item.

4.11.3.3 Method of automatic analysis. Once an optimum quality radiograph had been obtained, the image enhancement system began its automatic analysis. The first step was to scan the radiograph with a Sierra Scientific LSV TV camera, 1.5. The resulting video output was digitized by a Biomation A/D converter, and the digitized image was stored in the computer memory as a 512 x 512 pixel (picture element) array - each pixel quantized to one of 512 gray shades (from black at 0, to white at 511). The radiograph was thus converted into a form that the computer could manipulate and analyze. See Figure 5 (given as Figure 1 by Jacoby[9]). The contrast of the digitized image was then stretched to accommodate the full gray scale range. (This was a simple proportioning operation). See Figure 6 (given as Figure 2 by Jacoby[9]).

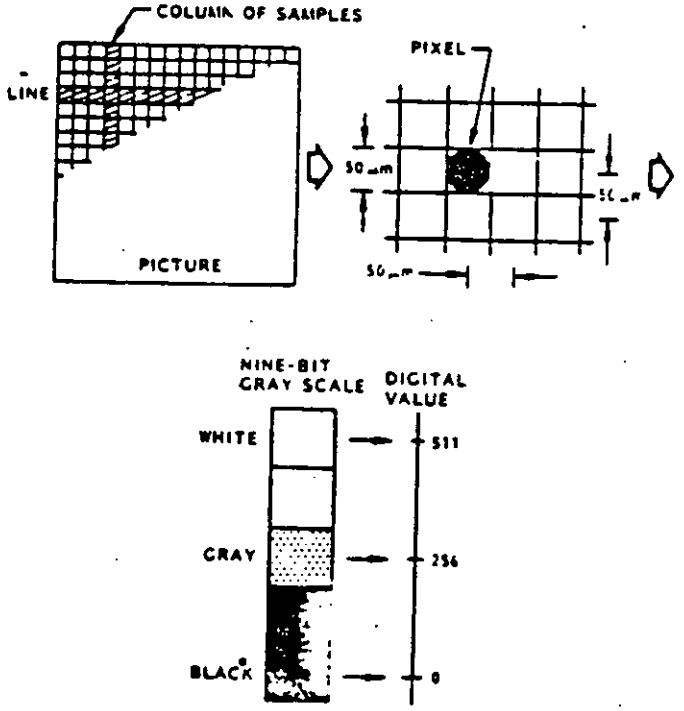

FIGURE 5. Sampling and Digitizing an image.[9]

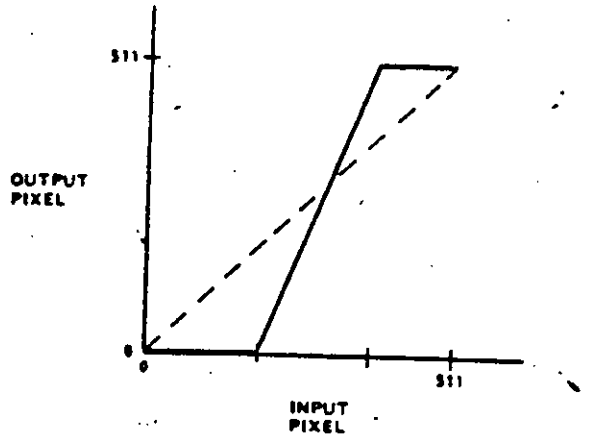

FIGURE 6. Contrast stretching.[9]

4.11.3.4 Removal of unwanted features. Since unwanted noise signals were introduced by the TV camera preamp and increased exponentially with optical density on the radiograph, they had to be minimized by "smoothing" the digitized image using low-pass filtering. That is, the effect of random noise was statistically nullified by producing a second 512 x 512 pixel array where each new pixel, e', was assigned a new gray scale value taken as the average of its former location value, e, averaged with those of its eight adjacent pixel neighbors. See Figure 7 (given as Figure 3 by Jacoby[9]). It was also pointed out how another troublesome feature, image density gradient, which occurs in radiographs of complex shaped specimens, could be removed by curve fitting and rescaling. The technique, called "field-flattening", fits a polynomial to the observed image density gradient, subtracts the original and fitted curves, and displays the remainder which results in a mapping of defect locations. See Figure 8 (given as Figure 4 by Jacoby[9]). The process is performed on a line-by-line basis over the whole x-ray image and demonstrates the extraordinary value and capability of the computer.

4.11.3.5 Thresholded image. After the field-flattening process, the image was then "thresholded" to locate flaws such as voids, cracks and porosity; i.e., after some preliminary statistics had been calculated, a square window size (typically 35 x 35 pixels) was arrived at through which pixels were observed as a group or array. The window size was set so that approximately 10% (statistically) of the pixels were below a certain threshold density. Each array of pixels which was below the threshold density was labeled a candidate flaw pixel. In this particular candidate pixel array, all pixels below the threshold were turned into a white binary image (marked 511), and all pixels above the threshold were turned into a black binary image (marked o). See Figure 9 (given as Figure 5 by Jacoby[9]). This technique highlighted

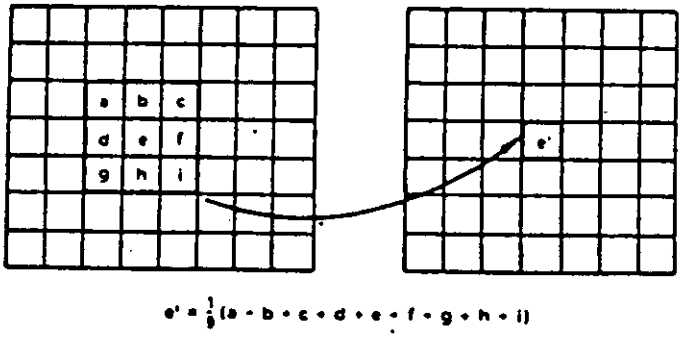

FIGURE 7. Low-pass filtering. The value of pixel e is replaced by e' calculated as shown[9]

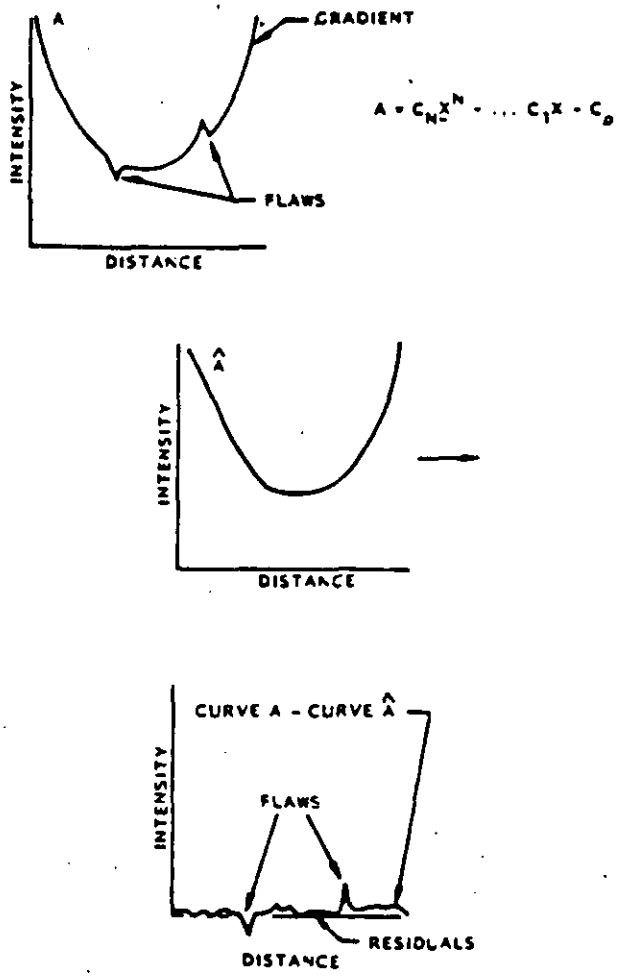

FIGURE 8. Field flattening.[9]

FIGURE 9. Thresholding[9]

the candidate array in full contrast. (If white pixels overlapped row-to-row vertically or horizontally, the entire 35 x 35 pixels were grouped together as one defect group and imaged white; if not, the entire array was imaged as some weighted gray tone). See Figure 10 (given as Figure 6 by Jacoby[9]). The defect candidates had thus been judged and imaged as enhanced flaw locations. This was done over the entire radiograph on a window-by-window basis to produce a binary image.

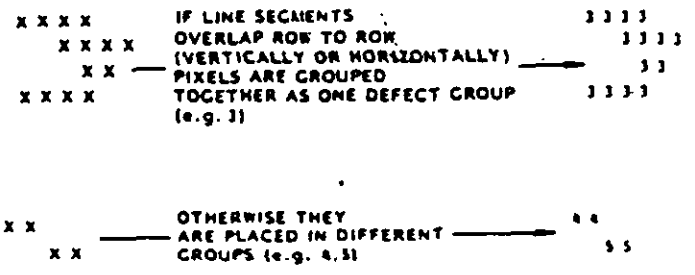

FIGURE 10. Grouping flaw pixels by line overlap.[9]

4.11.3.6 Automatic analysis of film. In the final step, the flaw sizes (adjacent areas of white defect group locations) were measured by the computer and a report was printed out. The report listed the number of flaws falling within specified flaw size ranges. The results were compared against predetermined specifications, and the specimen was either accepted or rejected by the computer. The radiographer simply positioned the film on the light table under the TV camera and instructed the computer where to search. Control then reverted to the computer, and the analysis of the film was done automatically.

4.11.4 Pressure vessel study. In another similar paper,[10] Jacoby describes an investigation of a glass-wrapped, rubber insulated, cylindrical pressure vessel. In this investigation, field flattening was performed to eliminate the density gradients caused by the cylindrical shape of the specimen. This was followed by a specially developed spacial filtering technique using Fourier analysis to decompose the two-dimensional matrix of brightness values that represents the image into a linear combination of elementary functions. The filtered spectrum is then transformed back into the image domain to clearly reveal cuts in the rubber insulation. The image was then smoothed to reduce noise indications and to permit efficient evaluation by the computer. In this way, a small vertical cut on the left-hand side of the filtered image and a high-density inclusion (neither of which were perceived on the original radiograph) became apparent.

4.11.5 Enhanced images in carbon-fiber-reinforced epoxy composite. In another report, Roberts and Vary[11] described the computer facility at the NASA-Lewis Research Center and how it was used to provide enhanced radiographic images in near real time of a carbon-fiber-reinforced epoxy composite fan frame ring for an aircraft gas turbine. The results of inspections by ultrasonic C-scan and paper radiography were also shown. The two methods of digital image enhancement used were brightness (or contrast) expansion and high-pass filtering. These were not applied to a radiograph, but to a thin-film radiographic sensing search which sensed an x-ray field at one face and displayed a visible image on its opposite face. A television camera accepts the visible radiation, converts it to a standard television signal, and passes it on to the computer for image enhancement.

4.11.5.1 Ultrasonic C-scan vs electronic image. The ultrasonic C-scan showed only the extent of delamination damage, while the radiograph clearly delineated the damaged areas. The electronic images showed the same damaged areas as the radiograph, as well as subtle variations in the damaged zones that were not evident in the radiograph.

4.11.5.2 Advantage of digital image analysis. This preliminary study showed that digital image analysis offers the advantage of immediate results, while revealing radiographic information that would not otherwise be evident in a conventional radiograph. Two types of irregularity were evident in the multi-ply composite element. One was major mechanical damage producing broken fibers and separated plies. The other was the junction of differently-oriented plies. For these types of irregularities in this type of material, computer-assisted radiographic inspection was clearly superior to either ultrasonic C-scan or film-based radiography.

4.11.6 Another study -- film image vs visual fluoroscopy. In another report, Yakushev and Dolmatovski[12] used an x-ray fluoroscopic (visual) and photographic method to monitor erosion-resistant asbestos plastic articles for nonuniform reinforcement distribution, voids, differences in resin content, and degree of cure. Low kilovoltage, soft x-radiation was used to produce images on both high-contrast (slow) film, and on a visual fluorescent screen with a magnification of 1.5. In this investigation, the film images were found to be superior to the visual fluoroscopic examination, revealing structural inhomogeneities and regions of differing binder concentration, whereas the visual fluoroscopic screens revealed only the structural inhomogeneities.

4.11.7 Conclusions of another study. In another report, Holloway, Shelton and Mitchell[13] have overviewed the field of radiographic image processing. They concluded that trade-offs may exist between resolution, sensitivity and speed. Whatever trade-off is made, the improvements frequently come at the expense of greater initial capital investment.

4.11.7.1 Results of study. The results of their paper suggest several potential advantages of image processing.

1) greater operator convenience and less fatigue,
2) less time between the discovery of an anomaly and initiation of corrective action,
3) decreased direct inspection cost,
4) fewer rejects at later stages of production run.
5) The greatest disadvantage is the increased cost of the equipment.

4.11.8 Further study. Another report by Johnson[14] on the use of computer-based radiographic inspection emphasizes that this type of process reduces corrective response time sufficiently to close the loop in a manufacturing-inspection process at minimal loss of sensitivity. Furthermore, Johnson demonstrated that it is neither necessary nor desirable to reject all but flaw-free products. Economics dictates that discontinuities smaller than some limit-value should not be rejected. Thus, the major reason for introducing a computer into the inspection process is to reduce variability, not necessarily to increase sensitivity.

4.12 Stereoradiography.

4.12.1 Determination of depth of a defect. In order to determine the depth of a flaw within a specimen, a number of stereo methods have been devised. These methods involve the making of a pair of radiographs of the same specimen, but with the tube head either shifted laterally or rotated with respect to the perpendicular to the film plane. These radiographs are then examined simultaneously and, with suitable markers placed on the specimen surface, the depth location of the defect within the specimen can be determined.

4.12.2 Description of method -- no depth perception. In one of these methods, commonly termed stereoradiography, two radiographs are made from two positions of the x-ray tube separated by a nominal inter-eye distance. The radiographs are then viewed with a stereoscope, a device which permits the left eye to see only the left eye position radiograph and the right eye to see only the radiograph made in the right eye position. With this viewing

technique, the brain causes the image to be seen in its correct 3-dimensional spacial relationship, as with normal vision, and defects are seen to stand out. This method, however, does not readily afford an actual depth measurement of a defect, but serves to provide spacial visualization.

4.12.3 Description of method -- depth measurement. With another technique, termed double-exposure or parallax method, an actual depth measurement can be made. In a recent report by Martin, Moore and Tsang,[15] a double-exposure method was used to measure the depth location of boron filament defects in a metal matrix composite. In order to obtain clear filament definition, a narrow-beam microradiography technique was used to make a stereographic pair of radiographs taken at known offset angles to the titanium-boron specimens. Using the measured shift of a known marker location, the depth of the defect was calculated by triangulation. Figure 11 (given as Figure 3[15]) clearly illustrates the derivation and set-up used in making the two triangulation radiographs from which the measurements for the defect depth determinations (S_e E) were made. The 20° triangulation angle was a nominal value selected to minimize the effect of errors in setting up the equipment. A small source-to-film distance was selected to reduce exposure time. A marker was made from 0.002-in. thick tantalum foil. Distance measurements were made at 100X magnification with a microscope equipped with filar eyepiece. From these measurements, the distances I'_e I'_m and I_e I_m could be computed.

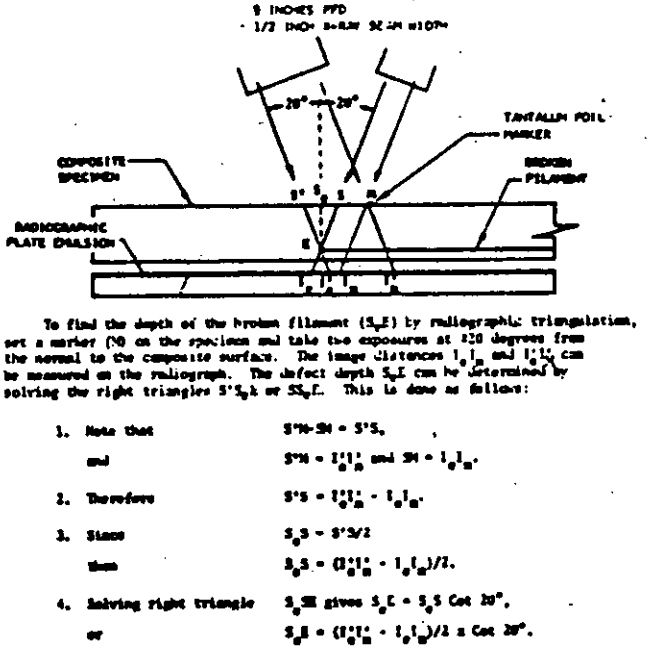

To find the depth of the broken filament (S_eE) by radiographic triangulation, set a marker (M) on the specimen and take two exposures at ±20 degrees from the normal to the composite surface. The image distances $I_eI'_e$ and $I_mI'_m$ can be measured on the radiograph. The defect depth S_eE can be determined by solving the right triangles $S'S_eA$ or SS_eE. This is done as follows:

1.	Note that	$S'M - SM = S'S_e$,
	and	$S'M = I'_eI'_m$ and $SM = I_eI_m$.
2.	Therefore	$S'S_e = I'_eI'_m - I_eI_m$.
3.	Since	$S_eS = S'S/2$
	then	$S_eS = (I'_eI'_m - I_eI_m)/2$.
4.	Solving right triangle	S_eSE gives $S_eE = S_eS \cot 20°$,
	or	$S_eE = (I'_eI'_m - I_eI_m)/2 \times \cot 20°$.

FIGURE 11 Derivation of relationship for determining defect depth[15]

4.12.3.1 Results. From the results obtained, the authors calculated the defect depth to be 0.009 inch. The composite had been fabricated using four layers of 4-mil boron filaments alternately sandwiched between five 0.0008-in. thick titanium alloy sheets. After diffusion bonding, the composite thickness was 0.045 in., which gives a nominal thickness of 0.009 in. for each layer; thus the defect was located in the first filament layer under the x-ray entry surface.

4.13 Opaque additives and image enhancement.

4.13.1 General. In an early work by Shelton,[16] significant improvements were made in image quality and sensitivity by impregnating subject materials with contrasting liquids, such as tetrabromethane (TBE), to increase image definition of voids and small cracks in graphite and to provide clearer weave patterns in composite materials.

4.13.2 Difficulties of graphite examination. The radiography of graphite presents certain difficulties; at x-ray energies where differential absorption is greatest, graphite, because of its low atomic number (Z), is more effective as a scatterer than as an absorber of radiation. Therefore, the processes of scatter and absorption occur at the same time and are in conflict. This difficulty becomes even more pronounced as the graphite shapes become more complex. Radiographic images of graphite rocket nozzle inserts, nose tips, nose cones, etc., are often unclear and lack sharpness around the edges. To overcome this problem, one approach taken by Shelton was to impregnate the materials with a solution of a higher atomic number compound so that differential absorption of the x-rays would improve the contrast on the resultant radiograph, and greater resolution of the structure of the material would be obtained. Tetrabromethane (TBE) was selected for this work.

4.13.2.1 Impregnation procedure. Multidirectional carbon/carbon composites and graphite of various thicknesses were used as the materials to be impregnated. The impregnation procedure involved four basic steps:

1) Preparation of the specimen by removal of moisture and surface contamination.
2) Contacting, as by soaking or sponging the specimen with tetrabromethane solution for a period of time sufficient to allow the TBE to penetrate into the cracks or voids present in the specimen.
3) X-raying the impregnated specimen.
40 Removal of the impregnant from the specimen.

4.13.2.2 Results. The time required for impregnating the piece to be inspected depends upon the thickness and the porosity of the material. The TBE can be completely removed from the impregnated article by evaporation with heat and pressure. A well ventilated area is necessary because TBE is toxic. Demonstration of the practical application of this technique was accomplished on eleven three-D multidirectional carbon/carbon rocket nozzle inserts. The radiographs of the impregnated inserts were much clearer and contained more detail, revealing the presence of cracks and pores that were not discernible when TBE was not used. Even the multidirectional nature of the laminated composite could be detected. Assurance that the TBE had been completely removed was obtained by radiographing an item before the TBE had been applied and after it was removed, and comparing the two radiographs. In general, therefore, the impregnation technique using TBE as an opaque additive gave much more detail to the shape of the pores and their interconnection. Other conditions, such as microcracks, were also made evident.

4.13.3 Graphite-epoxy composite investigation. In a graphite-epoxy composite investigation, Chang, Couchman et al [17] used the TBE opaque additive technique to monitor damage zone growth, matrix cracks parallel to fibers and delaminations between plies. A conventional x-ray technique is not suitable for the detection of delaminations in graphite-epoxy or carbon-epoxy composites, partly because carbon has a low attenuation coefficient for x-rays. Small differences in attenuation caused by planar delaminations and voids are indistinguishable on a radiograph. In this investigation, center-slit specimens were fabricated from Modmor II/Narmco 5208 graphite-epoxy laminates with orientations of (0/±45),(0/±45/90) and (±45). Tensile ramp and sawtooth cyclic loadings at different levels were applied to these specimens in an effort to correlate a failure mechanism with the level and mode of loading by monitoring the real-time damage zone growth. The x-ray technique consisted of introducing the opaque additive, TBE, into a prepared center-slit opening in the specimen using a hypodermic syringe. As the stress level in the neighborhood of the slit area was increased by increasing load, the TBE in the slit opening tended to enter the voids and delaminations by capillary action. The additive was found to have no deleterious effect on the matrix and fibers. When the testing time exceeded 2 hours, it was necessary to reapply the TBE to compensate for evaporation loss.

4.13.3.1 Experimental results. The experimental results were presented in the form of a time-sequence of radiographs of damage zones and plots of the damage length as a function of stress level, see Figures 12 and 13 (given as

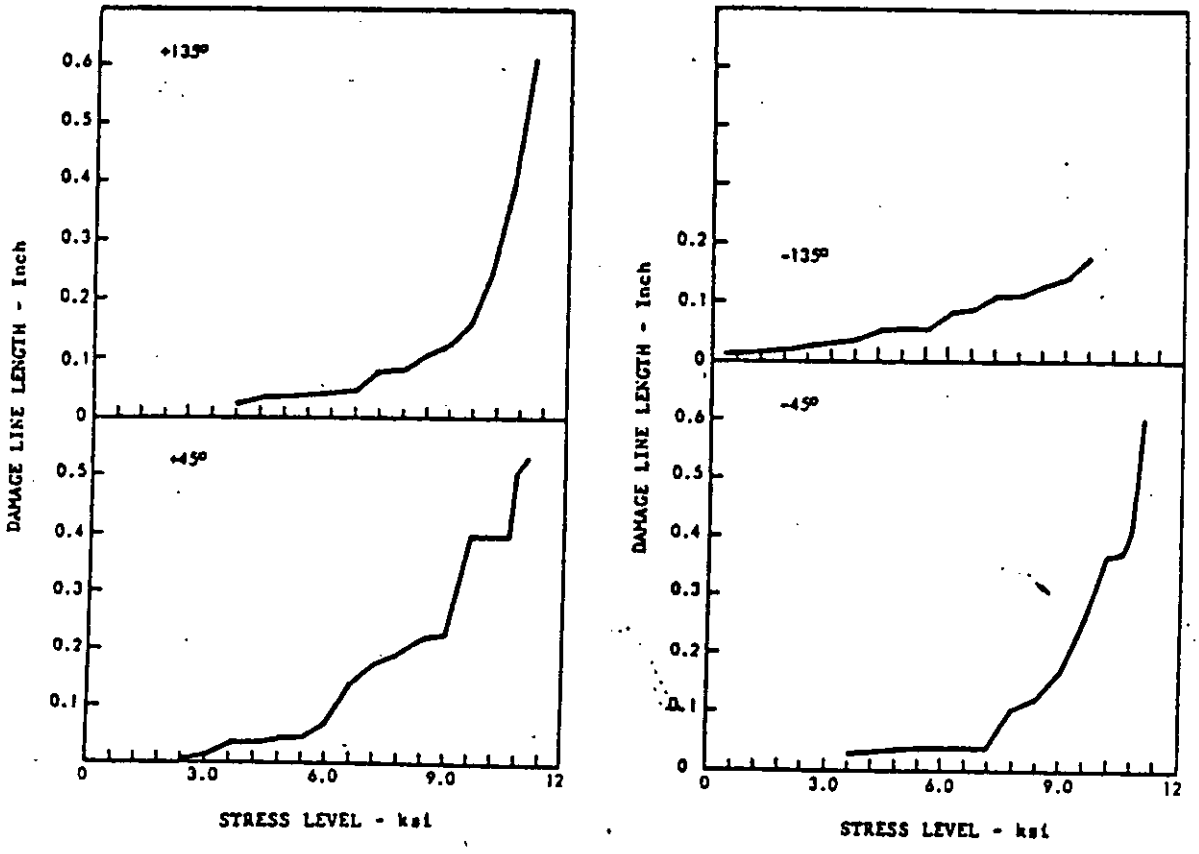

FIGURE 12. Damage line growth for a $[\pm 45]_{3s}$ specimen under ramp loading.[17]

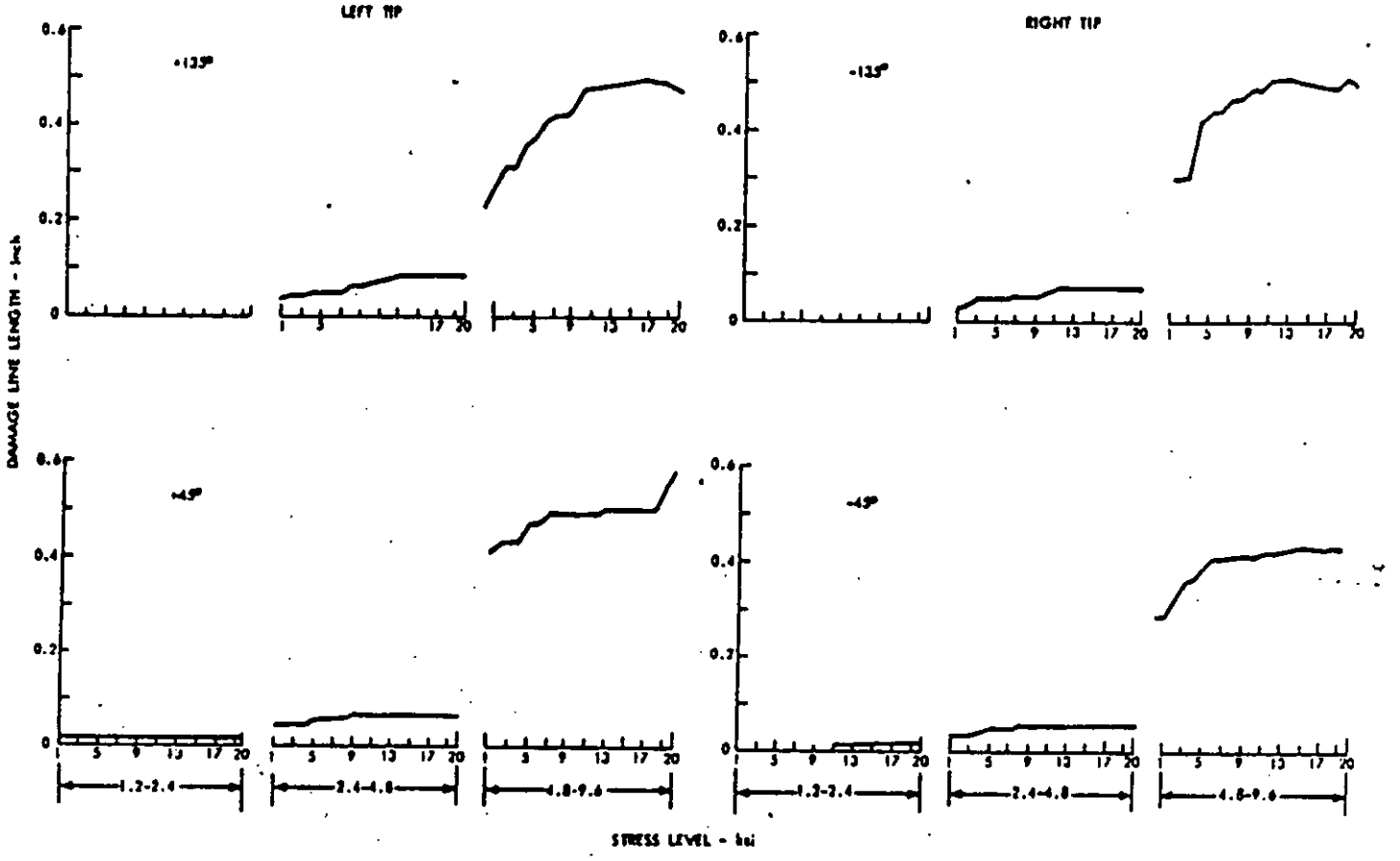

FIGURE 13. Damage line growth for a $[\pm 45]_{3s}$ specimen under cyclic loading.[17]

Figures 5 and 6 by Chang, Couchman et al[17]). It was established that this modified x-ray technique using TBE as an opaque additive can be very helpful in enhancing the radiographic image and in assessing the damage growth zone surrounding discontinuities in fibrous composite laminates. The method is efficient and can be economically applied in real time for stress concentration studies in composites. In addition, it was found that this technique can be used simultaneously with an acoustic emission monitoring technique for residual serviceability evaluation of composite components.

4.13.4 Addition of TBE to slits in the specimen. In a follow-up study of the same three types of graphite-epoxy composites, Chang, Gordon et al[18] employed the same technique of adding TBE to slits in the specimens to more fully characterize damage growth. Again, using specific tensile ramp loading and constant amplitude cyclic loading, it was evident that the main reason the specimen under cyclic loading could withstand higher stress was because sufficient time had elapsed for the load to be redistributed as the damage propagated.

4.13.4.1 Study of the failure mechanism. In addition, the failure mechanism for this type of composite was made observable by the introduction of TBE. Specifically, the question of whether matrix crazing or delamination between plies occurred first appeared to be resolved. It appeared that delaminations always originated from damage lines caused by matrix crazings. Once delamination started, the failure process would be accelerated until total failure occurred. The modified TBE x-ray technique also allowed the actual stress redistribution, characteristic of this type of laminate, to be observed.

4.13.5 Effect of TBE-enhanced inspection on fatigue life. In a related study, Sendeckyj[19] investigated the effect of TBE-enhanced x-ray inspection on fatigue life of graphite-epoxy composite specimens in order to either support or dispel fears of the unknown effects of the penetrant on the post-inspection behavior of these composites. He noted that some investigators had suggested TBE as being a good penetrant and, thus, a good wetting agent. Therefore, there exists the possibility that TBE may be absorbed by the resin leading to changes in the mechanical properties of the composite. Also noted was the existing possibility of dissociation of the TBE, leading to evolution of nascent bromine which is known to plasticize graphite fibers. Based upon a statistical analysis of the data obtained from the fatigue tests of graphite-epoxy specimens, Sendeckyj reported there is no statistical evidence for an effect of TBE-enhanced x-ray inspection on fatigue life of (± 45) graphite-epoxy.

4.13.6 Effect of DIB on compression fatigue life. In a similar study, Ratwani[20] investigated the unknown effect of diiodobutane (DIB) on the post-inspection compression fatigue life of graphite-epoxy laminates. Test specimens were fabricated from a $(0/\pm 45/90/0/\pm 45)$ laminate using the Hercules AS/3501-6 graphite-epoxy system with and without DIB. He concluded that DIB does not have any detrimental effect on the compression fatigue life of this type of composite under room temperature dry environments.

4.13.7 Comparisons of damage indications. In a more recent study by Sendeckyj, Maddux and Tracy,[21] side-by-side comparisons of damage indications obtained by using TBE-enhanced x-ray, through-transmission ultrasonic C-scan, and holographic nondestructive inspection methods on various composite specimens were presented and discussed. Specific results were presented for (a) graphite-epoxy specimens containing fatigue induced damage regions from surface notches and through-the-thickness circular holes and (b) hybrid composite specimens containing static loading induced damage regions near central through-the-thickness slits. The results showed that the TBE enhanced radiographic method gives the most detailed information on the nature and planar distribution of damage. It is capable of finding fiber fractures, matrix cracks and delaminations. The ultrasonic C-scans gave the least information. The holographic method, using thermal loading, provided information on delaminations near the specimen surfaces and cracks in the surface plies. This information, in conjunction with that provided by the TBE-enhanced radiographs, gave an accurate description of the damage region.

4.13.7.1 Recommendations. The authors also made the following recommendations: (1) an x-ray opaque fluid that is not as toxic as TBE should be found and used in future applications, and (2) a procedure for using enhanced radiographs for getting information on the through-the-thickness distribution of damage in composites should be developed. X-raying the specimen edgewise, making stereo-pair radiographs and constructing a three-dimensional x-ray image of the damage by using tomography were suggested as possibilities.

4.13.8 Radiographic stereo-mode image enhancement. In another study using opaque additives for radiographic stereo-mode image enhancement, Joiner[22] investigated carbon-epoxy specimens impregnated with molten sulphur to better reveal the extent and distribution of voids. Shear and transverse strength measurements were also made on the composites, and the effect of voids on these properties was investigated.

4.13.8.1 Technique. For the radiographic examination, the specimens were impregnated under vacuum with molten sulphur at 140°C for 4 hours. The specimens were than cooled and excess sulphur was removed using very fine emery paper to give a visually clean surface. The specimens were then radiographed in a light tight box by exposure to 12 kV x-rays for 30 seconds at a source-to-film distance of 25.4 cm and an offset angle of 11.5 degrees. The samples were then rotated 180 degrees and a second radiograph taken. This formed a stereoradiographic image pair allowing easy examination of the void distribution throughout the sample.

4.13.8.2 Results. This work indicates that the modified radiographic technique used is capable of determining the extent and distribution of voids in carbon-fiber composites. Voids of micron size were detected and their effects on composite shear and transverse strengths were demonstrated and explained. Joiner says that, if it can be established that sulphur impregnation does not have a significant effect on the composite properties, the present examination technique will be capable of extension to form the basis of a nondestructive testing technique for the quality control assessment of fabricated items.

4.13.9 Another image enhancement investigation. In another recent and somewhat imaginative image enhancement investigation by Crane, Chang and Allinikov,[23] it was shown that the addition of boron fibers to the edges of graphite-epoxy prepreg tapes facilitated the radiographic inspection of both the distribution and integrity of fibers on a tape-by-tape level within the component. The technique consisted of adding a boron fiber to the edges of each composite tape. This extra fiber was first coated with a dilute solution of the epoxy matrix and methyl ethyl ketone and then dusted with a powdered fluorescent dye to enhance its visibility. The coated fiber appeared as a distinct bright yellow line against the black background of the graphite tape (during fabrication) and would permit automated inspection of the tape position with simple optical readers.

4.13.9.1 Testing composite plate with boron fiber additions. Since the ability to radiographically see the individual tungsten cores of the boron fibers in thick laminates was open to question, a 50-ply thick composite plate with boron fiber additions was fabricated and examined. The plate was radiographed using 25 kV and 3 mA for 120 seconds on Type M Kodak film. Remarkably, almost all the boron fibers were clearly visible on the radiograph, except in a few cases of overlap. The tungsten core of the boron filament, since it is more radiographically opaque, permitted a tape-by-tape level examination for ply orientation and sequencing, fiber washing and waviness and ply overlap or underlap. A three-point bending test performed on the composite suggested that the small addition of the boron fibers did not effect the mechanical properties.

4.13.9.2 Use of boron marker fibers. The use of boron marker fibers would be limited in their application to composite structures where the radius of curvature is greater than approximately 0.635 cm, depending on the strength of the boron fiber used. Since the boron in the fiber is more dense to neutrons than the surrounding composite, it would also serve as a marker fiber for a neutron radiograph of the structure. Information concerning the internal structure of the composite could be easily obtained using this technique since the boron sheath of the fiber is larger by a factor of 40 than the tungsten boride core.

4.13.10 Assessing internal features. In a recent overview study by Prakash[24] on nondestructive testing of composites, a number of NDT techniques, including microradiography, were evaluated for their applicability to assess internal features such as voids, fiber volume fraction, fiber wash or misoriented fibers, interlaminar and translaminar cracks, lay-up orders, latent defects, etc. Prakash also commented on the use of opaque additives. The two types of composite samples used for this study were carbon fiber-reinforced plastics (cfrp) and glass fiber-reinforced plastics (grp). Cfrp samples were made with commercially available carbon fiber prepreg sheets containing HM-S (Type 1) carbon fibers in 828/DDM/$BF_3$400 epoxy resin and using a compression molding technique. Grp samples were made with E-glass fibers and epoxy resin by the hand lay-up method. The samples were made to deliberately contain a wide spectrum of internal defect features.

4.13.10.1 Radiographic studies. For the radiographic studies, a commercially available low voltage beryllium window x-ray generator was employed. For 2.5-mm thick cfrp laminates, good radiographs were obtained using a 7 minute exposure time with 12 kV and 0.5 mA.

4.13.10.2 Types of discontinuities found with radiography. It was found that radiographs provide a good overall view of frp laminates under inspection (e.g., general fiber orientation, fiber wash or misorientation, fiber kinks or wrinkles, etc.) and foreign objects or inclusions are easily detected. Cracks aligned parallel to the direction of x-ray beam travel (i.e., translaminar cracks) are also readily revealed. Thermal or shrinkage cracks are generally present in the form of translaminar cracks, especially in cross-plied cfrp laminates, because of the thermal anisotropy of various prepreg layers. These cracks can best be detected using an x-radiography technique.

4.13.10.3 Types of discontinuities not found with radiography. It was also determined in this study that x-radiography does not appear suitable for the measurement of fiber volume fraction. Interlaminar defects, such as voids, do not have an appreciable dimension in the direction of x-ray beam travel and are therefore not detectable by this technique.

4.13.10.4 Radiography using newer techniques. Prakash concluded his discussion on radiography of composites by commenting on the feasibility of some of the recently developed techniques. Regarding the use of a sulphur penetration technique to enhance void images, he notes that the rate of sulphur penetration into microvoids in large structures may be too slow to be of any use on economical grounds, and that the effects of sulphur impregnation on the mechanical properties has not been established and may prove to be impractical. In reference to the impregnation of delaminated specimens with a dense filler (lead oxide in a gelatin) to obtain radiographs which provide an indication of the degree of delamination cracking, Prakash notes that total penetration of the crack cannot be guaranteed.

4.13.10.5 Use of tracer filaments. He also notes that, if tracer filaments of high density (such as lead silicate) are introduced while making the laminate, it may be possible to follow the lay-up, but that the results obtained cannot be totally relied upon because tracer fibers may not move in the same manner as the surrounding fibers.

4.13.10.6 Establishing fiber orientation. Prakash notes that the technique of microradiography or x-ray microscopy, which consists of cutting a very thin slice of any sample, obtaining a radiograph, and subsequently optically enlarging the radiograph, has also been used to establish fiber orientation, etc., in grp and cfrp samples, but that it is difficult to visualize how this technique could be applied on a production scale.

5.0 Neutron radiography

5.1 General. Neutron radiography, like x- or gamma radiography, depends upon the differential absorption of neutrons by the specimen material. However, while x-rays interact with the atomic orbiting electrons, neutrons interact with the atom's nucleus. There is no well-ordered relationship between neutron absorption and scattering coefficients and material atomic number as there is for x-rays (where absorption and scatter generally increase with atomic number). Neutrons, particularly those with low velocities (thermal neutrons), exhibit a random variation of absorption from element to element. The range of absorption coefficients for neutrons is 0.03 to 90, considerably exceeding that for x-rays (0.13 to 4.0), which allows for greater flexibility and excellent contrast in neutron radiographs. Furthermore, elements with adjacent atomic numbers may have widely different neutron absorption coefficients, and some low atomic number elements (such as hydrogen) can attenuate neutrons much more strongly than some high atomic number elements (such as lead). Thus, thicker sections of high atomic number materials can be radiographed with neutrons in a much shorter time than with x- or gamma rays. Also, neutron radiographs can exhibit a sharp contrast between elements which have similar absorption coefficients for x- or gamma rays but quite different ones for neutrons, such as boron and carbon, cadmium and barium.

5.2 Use of converter foils. Unfortunately, however, since neutrons are uncharged particles, they exhibit negligible direct photographic effects on film, and neutron energy must be somehow converted to produce a radiographic image. Two techniques using converter foils are presently employed to accomplish this. The first technique is direct exposure wherein the film is sandwiched between two layers of foil (gadolium, rhodium, indium or cadmium) and exposed. The foils become radioactive when exposed to the neutrons and emit beta or gamma radiation which, in turn, expose the film to produce an image. The second technique is a transfer exposure method wherein the converter foil alone is exposed to the neutron radiation passing through the specimen. The radioactive foil is then placed in intimate contact with the film for sufficient time to expose the film and produce an image. Converter foils of gold, indium and dysprosium have been used in this technique.

5.3 Sources of neutrons. The most common source of neutrons for neutron radiography is a nuclear reactor which provides a horizontal beam of thermal neutrons of high intensities but limited to only a few inches in diameter. This permits short exposure times but may require numerous radiographs for imaging large objects. Neutron beams which do not spread significantly and which contain few gamma rays are desirable for promoting high resolution in the radiographic image. Electronic and isotopic sources (such as californium-252) of neutrons are also available.

5.4 Use of neutron radiography. While neutron radiography is most frequently used when x- or gamma ray techniques are unable to perform a desired inspection task, it is also considered a useful complement to those techniques. For example, the detection of hydrogen pockets within a metal container is readily made by neutron radiography. Other applications include the inspection of brazed joints, tires, printed circuits and the location of core materials in investment castings.

5.4.1 Other uses. Neutron radiography is being explored as an inspection tool for numerous composite materials such as boron fiber-aluminum, boron-epoxy or bonded honeycomb structures. Neutron radiography is also being used together with x-radiography to inspect fiber-reinforced plastic composites, with resin voids being detected by the neutrons and fiber orientation by the x-rays. Bondline defects in certain adhesively bonded composite/metal structures have also been accurately and reliably inspected by neutron radiography.

5.4.2 Checking structural integrity. In a 1977 report, Dance and Petersen[25] used neutron radiography to inspect the structural integrity of adhesive bondlines between a laminated aluminum alloy skin and the rib/spar in an airframe wing box, see Figure 14 (given as Figure 2 by Dance and Petersen[25]). The laminated skin consisted of three 0.063-inch aluminum layers bonded to each other and to the rib/spar with 0.005-inch epoxy adhesive. The hydrogen content of organic materials, such as epoxy adhesives, typically ranges from 8 to 12 percent. It is readily evident, therefore, that even very thin bondlines can be easily imaged using neutron radiography. Furthermore, the neutron radiography technique is not troubled by discontinuities, such as those occurring at bondline overlap edges, as are acoustic and ultrasonic techniques. This is particularly important because of the nature of the stresses in the bonded joint. The edges should be the area of most effective inspection.

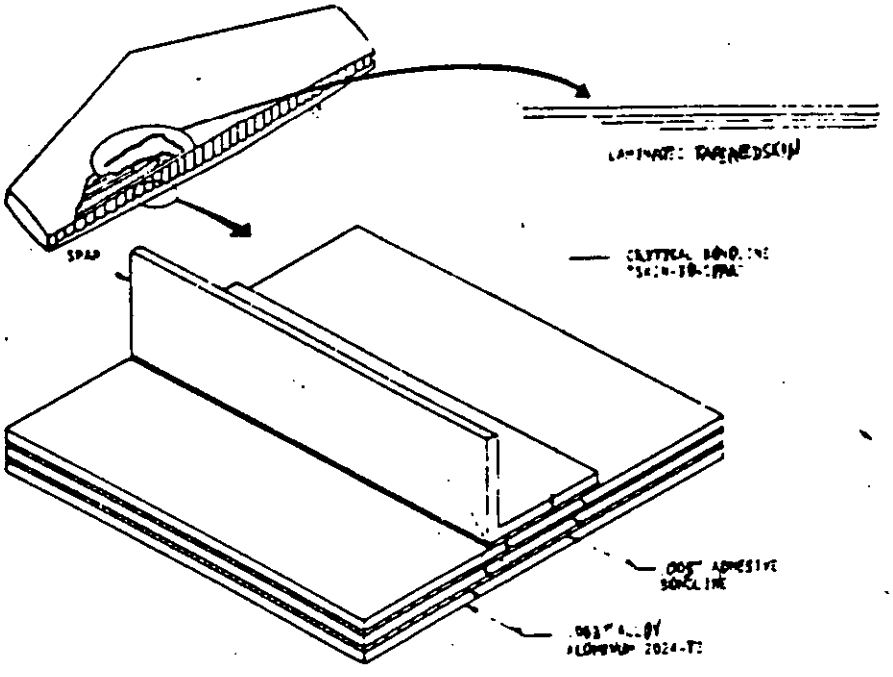

FIGURE 14. Adhesively-bonded primary structure test specimen.[25]

5.5 Use of image enhancement additives. The authors discussed their inspection for bondline voids and gross porosity using epoxy adhesives with and without neutron radiography image enhancement additives. The two adhesives investigated were Narmco 6800 and Hysol 9312. Both were used as received from the vendor and as modified by the addition of a gadolinium oxide neutron radiography image enhancer. A number of specimen assemblies were prepared to include a variety of void fractions by the addition of different amounts of acetone to the epoxy resins prior to adhesive application.

5.5.1 Method. Neutron radiographic inspection was performed using a 2.8 mg californium-252 source. The thermal neutron flux was approximately 10^4 n/cm^2-sec. Industrial x-ray film, types SR-54 and AA were used. A 0.001-inch-thick vapor-deposited gadolinium metal film was used as a converter, see Figure 15 (given as Figure 3 by Dance and Petersen[25]). In addition to neutron radiographic inspection, each critical bondline, between the laminated skin and rib/spar, was tested for strength in order to correlate observed void fractions and strength predictions. Radiographs were made of all the specimen assemblies and bondline voids were clearly visible in all cases. However, it was obvious that the gadolinium oxide image enhancer significantly improved the contrast whenever used.

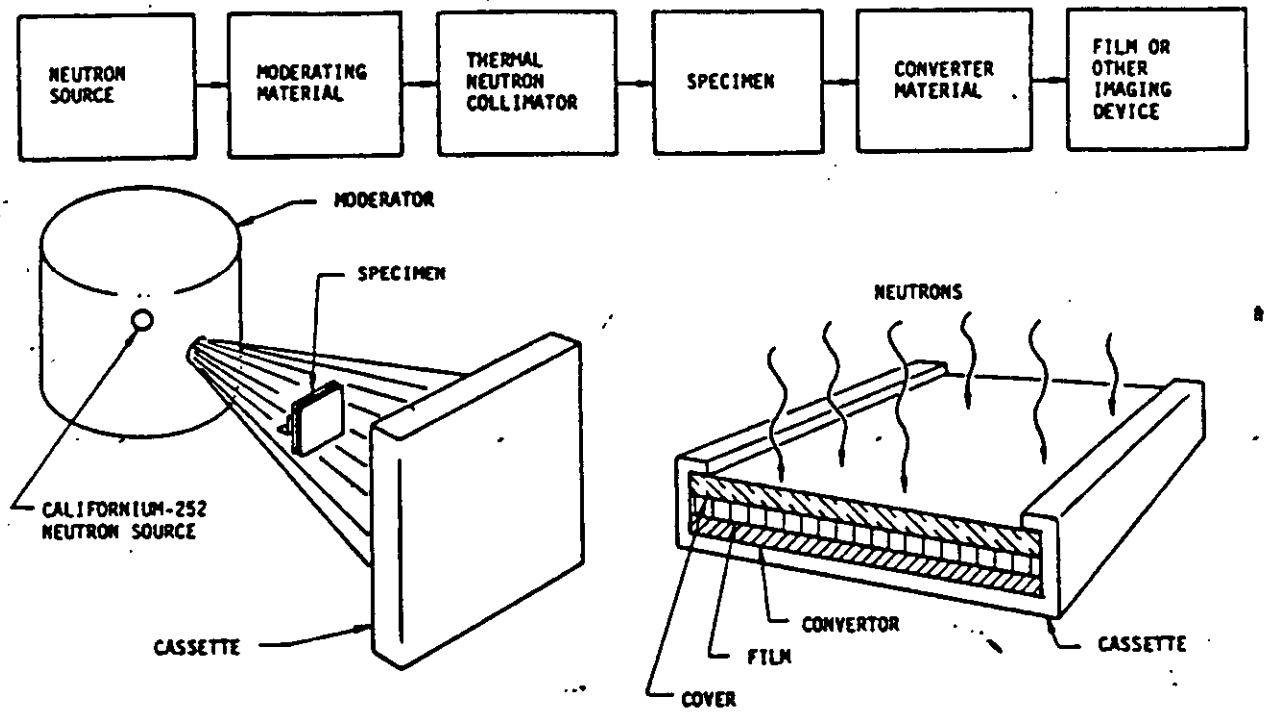

FIGURE 15. Neutron radiographic imaging.[25]

5.5.2 Results. From the data obtained, the authors concluded that the value of neutron radiography for assessing the serviceability of this type of laminated structure had been clearly demonstrated. They also concluded that the use of gadolinium oxide as an image enhancer greatly improves radiographic contrast and is effective for rapid inspection and strength prediction of adhesively bonded joints.

5.6 Study of penetrating radiation techniques. In an early preliminary study of penetrating radiation techniques for the inspection of multidirectional reinforced resin matrix composites, Cook and Gulley[26] investigated a number of techniques including neutron radiography, conventional film x-radiography and the x-ray Vidicom television imaging technique.

5.6.1 Samples. The composites investigated included a woven quartz fiber-phenolic resin flat panel which was approximately 30 inches long, 6 inches wide and 3/8 inch thick. All of the panels were evaluated by both conventional film x-radiography and neutron radiography. Since the composite matrix material was a phenolic resin which contained hydrogen atoms of high neutron capture cross-section, it was anticipated that neutron radiography would be a successful method for defect detection. Several composite samples were fabricated. Some were doped with paraffin and some with a gadolinium salt to enhance the absorption of neutrons. In addition, several small diameter flat-bottom holes were placed in some samples to simulate defects.

5.6.2 Comparison between doped and undoped samples. The neutron radiographs of the undoped composites were no better, and usually of poorer quality than the x-ray film of the same samples. Only the addition of a doping agent, particularly gadolinium nitrate, provided the contrast and density necessary for quality radiographs. Weave irregularities in the reinforcement were better evaluated by conventional film radiography.

5.6.3 Results. The authors concluded that, while further enhancement by doping may lead to improved analysis, neutron radiography must be considered of limited value for inspecting resin matrix composites. The disadvantage of utilizing a reactor source of neutrons also places restrictions on the potential application of this method.

5.7 Feasibility of measuring resin content. A recent report by Martin[27] concerned the feasibility of measuring composite resin content by radiographic (including gauging) techniques. The use of both low kV x-rays and thermal neutrons was also considered. In particular, Martin attempted to detect resin-rich or resin-starved areas caused by porosity and curing variables. It was assumed that the x- or neutron radiation interacted only with the resin and fibers, and not the porosity.

5.7.1 Samples. Graphite fiber (Thornel 300) reinforced epoxy resin (Narmco S208) composite test panels (0.25" x 4" x 10") were fabricated from prepreg tape approximately 2" wide and 0.005" thick.

5.7.2 Results. Based upon calculations of the composite mass absorption coefficient versus resin content for both x-rays and neutrons, and upon roughly equivalent experimental data, Martin concluded that the use of x-rays for measuring composite resin content is not feasible because of insufficient sensitivity for detecting small changes in composite density and mass absorption coefficient due to variations in resin content. Although changes in the neutron mass absorption coefficient due to changes in the resin content are significantly larger than the corresponding situation for x-rays, Martin also concluded that the neutron film technique is not sensitive enough for practical measurement of resin content. Martin also concluded that the use of neutron gauging is feasible for detecting changes in resin content of $\pm$ 1 percent, but that further experimental work would be necessary to determine the practicality of using neutron gauging for measuring composite resin content.

5.8 Inspection of fiberglass composites. In a 1972 report by Youshaw[28], the feasibility of applying neutron radiography to the inspection of massive fiberglass composites was studied. There are several manufacturing anomalies, such as resin-rich regions, which are thought to be beyond the limits of ordinary x-radiography and the other tools of nondestructive testing. In view of the low atomic numbers of the resin constituents in composites and the large cross section for reaction with neutrons for these elements, Youshaw determined that abnormalities such as resin-rich regions could be expected to react with a neutron beam.

5.8.1 Method. Fiberglass sonar domes were fabricated manually by applying successive layers of resin-impregnated strips of glass fibers to a female mold, and squeezing the strips to remove entrapped air. For the neutron radiography work, gadolinium screens were selected for the prompt emission technique and indium screens for the transfer or induced method of obtaining an image.

5.8.2 Results. Youshaw summarized that this study showed that the boron constituent of the fiberglass severely attenuated neutrons at thermal energies, necessitating long exposure times to obtain film darkening. Simultaneously, the hydrogen of the binding resin very efficiently scattered neutrons, which acted to fog the film. Considering the thickness of the sonar domes, Youshaw concluded that neutron radiography is not a suitable inspection tool for this item. Furthermore, it was demonstrated that conventional x-radiography can be usefully applied.

6.0 NOTES

6.1 Conversion factors. When metric units are required, units for inch may be converted to the metric equivalent as follows:

English	Multiply by	Equals	Metric unit
inch	2.54	=	centimeter (cm)

6.2 Subject term (key word) listing.

Nondestructive Testing
Composite Materials Testing
Radiography of Composite Materials
Radiography

Custodians:

Army -- MR
Navy -- AS
Air Force -- 20

Review activities:

Army -- MI, AV, AT, AR, AS
Navy -- OS
Air Force -- 99, 84, 82, 80

User:

Army -- ME
Navy -- SH

Military Coordinating Activity:

Army -- MR

Project No. NDTI-0115

WP# ID-6984A/DISC-0520A. FOR AMMRC USE ONLY.

LITERATURE CITED

1. OWSTON, C.N., and CONOR, P.C. Failure Mechanism in Carbon Fiber Reinforced Polymer and Their Relation to Non-Destructive Testing. Composites, September 1970, p. 268-276.
2. RODERICK, G.I., and WHITCOMB, J.D. X-Ray Method Shows Fibers Fail During Fatigue of Boron-Epoxy Laminates. J.Comp. Mat., v. 9, October 1975, p. 391-393.
3. RODERICK, G.I., and WHITCOMB, J.D. Fatigue Damage of Notched Boron/Epoxy Laminates Under Constant Amplitude Loading. N77-17165/OST, Report No. NASA-TM-X-73994, December 1976.
4. ARTIS, L.J.,and JOINER, J.C. Methods of Measurement of the Relative Performance of Various Classes of Resins in Carbon Fibre Composite. N73-31536/8, Report No. AQD/NM-000198, October 1972.
5. HUGGINS, B.E. Radiography with Low Energy Radiation, Brit. J. of NDT, May 1981, p.119-125.
6. MARCUS, L.A., and STINCHCOMB, W.W. Measurement of Fatigue Damage in Composite Materials. Exp. Mech., v. 15, no. 2, February 1975, p. 55-60.
7. DARLINGTON, M.W., and McGINGLEY, P.L. Fibre Orientation Distribution in Short Fibre Reinforced Plastics. J. of Mater.Sci., v 10, 1975, p. 906-910.
8. VARY, A. Investigation of an Electronic Image Enhancer for Radiographs. Mater.Eval., December 1972, p. 259-267.
9. JACOBY, M.H. Nondestructive Testing of Composites. Proc. of the Inst. of Environmental Science, Tech Paper, Lockheed Missiles and Space Co., Sunnyvale, California, 1980.
10. JACOBY, M.H. Image Proceeding for Nondestructive Evaluation. Tech. Paper, Lockheed Missiles and Space Co., Sunnyvale, California, 1980.
11. ROBERTS, E., and VARY, A. Inspection of Composites Using a Computer Based Real Time Radiographic Facility. NASA-TM-X-73504, 1976.
12. YAKUSHEV, V.F., and DOLMATOVSKI,M.G. Monitoring the Quality of Asbestos Plastics by an X-Ray Method. Sov. J. NDT, v. 10, no 6, November - December 1974, p. 727-729.
13. HOLLOWAY, J.A., SHELTON, W.I., and MITCHELL,J. Image Processing of Industrial Radiographs. AFML-TR-75-46, March 1975.
14. JOHNSON, D.P. Inspection Uncertainty: The key Element in NondestructiveInspection. Mater. Eval., v. 34, no. 6, June 1976.
15. MARTIN G., MOORE, J.F., and TSANG, S. The Radiography of Metal Matrix Composites: Mater. Eval., April 1972, p.78-86.
16. SHELTON, W.L., Improved Radiographic Techniques for Graphite and Carbon/Carbon Composite Materials. Proc. 8th Symp. on Nondestructive Evaluation in Aerospace Systems and Nuclear Applications, San Antonio, Texas, April 1971, p. 134-154.
17. CHANG, F.H., COUCHMAN, J.C., EISENMANN, J.R., and YEE, B.G.W. Application of a Special X-Ray Nondestructivce Testing Technique for Monitoring Damage Zone Growth in Composite Laminates. ASTM-STP 580, 1975, p. 176-190.
18. CHANG, F.H., GORDON, D.E., RODINI, B.T., and MC DANIEL, R.H. Real-Time Characterization of Damage Growth in Graphite/Epoxy Laminates, J. Compos. Mater., v. 10, July 1976, p. 182-192.
19. SENDECKYJ, G.P. The Effect of Tetrabromethane-Enhanced X-Ray Inspection on Fatigue Life of Resin-Matrix Composites. Compos. Tech. Review, v. 2, no. 1, Winter 1980, p. 9-10.
20. RATWANI, M.M. Influence of Penetrants Used in X-Ray Radiography on Compression Fatigue of Graphite/Epoxy Laminates. Compos. Tech. Review, v. 2, no. 1, Winter 1980, p. 10-12.

21. SENDECKYJ, G.P., MADDUX, G.E. and TRACY, N.A. Comparison of Holographic, Radiographic, and Ultrasonic Techniques for Damage Detection in Composite Materials. Proc. of 1978 Int. Conf. on Composite Materials, Toronto, Canada, April 1978. p. 1037-1056.
22. JOINER, J.C. The Determination of Voids in Carbon Fibre Composites. Report AQD/NM-000296, 1974.
23. CRANE, R.L., CHANG, F. AND ALLINIKOV, S. The Use of Radiographically Opaque Fibers to Aid the Inspection of Composites. Mater. Eval., v. 36, no. 10 September 1978, p. 69-71.
24. PRAKASH, R. Nondestructive Testing of Composites. Composites, October 1980, p. 217-224.
25. DANCE, W. E. AND PETERSEN, D.H. Verification of the Structural Integrity of Laminated Skin-to-Spar Adhesive Bondlines by Neutron Radiography. J.Appl.Polymer Sci, Applied Polymer Symposium 32, 1977, p. 399-410.
26. COOK, J.L. and GULLEY, L.R. Penetrating Radiation Inspection of Multidirectional Reinforced Resin Matrix Composites. Materials 1971 Proc., 16th Nat. Symp. Soc. Aerospace Materials and Process Eng., Anaheim, California, April 1971, p. 345-354.
27. MARTIN, B.G. An analysis of Radiographic Techniques for Measuring Resin Content in Graphite Fiber Reinforced Epoxy Resin Composites. Mater. Eval., v. 35, no. 9, September 1977, p. 65-68
28. YOUSHAW, R.A. Neutron Radiography of Massive Fiberglass Composite Structures Feasibility Study. AD-752 457, 1972.

BIBLIOGRAPHY

Typical Applications

ALLEY, B.J. X-Ray Fluorescence Analysis of Composite Propellants for Army Missile Systems. AD-A044 686/4st, June 1977.

ASHLEY, D.G. Measurement of Glass Content in Fibre/Cement Composites by X-Ray Fluorescence Analysis. NDT International, April 1979, p. 56-60.

AWERBUCH, J and HAHN, H.T. Hand Object Impact Damage of Metal Matrix Composites.J. Compos. Mater., v. 10, July 1976, p. 231-257

BAILEY, C.D., FREEMAN, S.M. and HAMILTON, J.M. Detection and Evaluation of Impact Damage in Graphite/Epoxy Composites. Mater. and Processes in Service Performance Soc. for Adv. of Mater. and Processing Eng., 9th Tech. Conf., Atlanta, Georgia, October 1977. p. 491-503.

BASLER, G., HAMBURG, A. and SCHMEISSER, H. Radiometric Inspection of Glass Fibre Reinforced Pipes by Means of an Image Analyzing System. Materialpruefung, v. 19, no. 9, 1977, p. 361-365.

BAYLAS, E. Radiographic Testing of Glass Fiber Reinforced Plastic Material. AD-312991, 1976.

BREWER, W.D. and KASSEL, P.C. Flash X-Ray Technique for Investigating Ablative Material Response to Simulated Re-Entry Environments. Int. J. of NDT, v. 3, 1972, p. 375-390.

COMPTON, W.A., STEWARD, K.P. and MNEW, H. Composite Materials for Turbine Compressors. AD-935 373, June 1968.

COOK, J.L., Multidirectional Fiber-Reinforced Resin Matrix Composites. AD-883 978/9st, February 1971.

COOK, J.L., REINHART, W.W. and ZIMMER, J.E. Development of Nondestructive Testing Techniques for Multidirectional Fiber-Reinforced Plastics. AD-746 592, 1971.

CRANE, R.L., Measurement of Composite Play Orientation Using a Radiographic Fringe Technique. Mater. Eval., v. 34, no. 4, April 1976. p. 79-80.

CRANE, R.L., Nondestructive Inspection of Composites and Adhesively Bonded Structures. AD-770 823, 1980.

CRISCUOLO, E. L. and POLANSKY, D. Application of Radiographic Specifications. Nondestructive Testing, v. 20, no. 2, March-April 1962, p. 114-118.

CROSSMAN, F.W. et al. Initation and Growth of Transverse Cracks and Edge Delamination in Composite Laminates, Part 2 - Experimental Correlation. J. of Compos. Mater. Supplement, v. 14, 1980.

DASTIN, S.J. and LUBIN, G. Adhesive Bonding High Modulus Composite Aircraft Structures. Adhesive Age, June 1971, p. 28-32.

EPSTEIN, G. Nondestructive Test Methods for Reinforced Plastic/Composite Materials. AD-696 466, February 1969.

EVANGELIDES, J.S., and MEYER, P.A. Investigation of the Properties of Carbon-Carbon Composites and Their Relationship to Nondestructive Test Measurements. AD-753 874/8st, August 1974.

FRENCH, C.R. Radiographic Examination of Large Filament-Wound, Solid-Propellant Motor Cases. Mater. Eval., v 24, no. 8, August 1966. p. 412-416.

GOSSE, H.J., KAITATZIDI, M., and ROTH, S. Testing Procedures for Carbon Fiber Reinforced Plastic Components. N77-30182/8st, July 1975.

HAGEMAIER, D.J. Bonded Joints and Nondestructive Testing. Nondestructive Testing, February 1972, p. 38-48.

HAGEMAIER, D.J. NDT of Aluminum-Brazed Titanium Honeycomb Structures. Nondestructive Testing (London), v. 9, no. 3, June 1976, p. 107-116.

HAGEMAIER, D.J., MC FAUL, H.J. and MOUA, D. Nondestructive Testing of Graphite Fiber Composite Structures. Mater. Eval, v. 29, no. 6, June 1971, p. 133-140.

HAGEMAIER, D.J., MC FAUL, H.J. and PARKS, J.T. Nondestructive Testing Techniques for Fiberglass, Graphite Fiber and Boron Fiber Composite Aircraft Structures. Mater. Eval., v. 28, no. 9, September 1970, p. 194-204.

HASTINGS, C.H. AND GRUND, M.V. Radiographic Inspection of Reinforced Plastics and Resin-Ceramic Composites. Nondestructive Testing, v. 19, no. 5, September-October 1961, p. 347-351.

HENDRON, J.A., GROBLE, K.K. and WANGARD, W. The Determination of the Resin-to-Glass Ratio of Glass-Epoxy Structures by Beta Ray Back Scattering. Mater. Eval., v. 22 no. 5, May 1964, P. 213-216.

JONES, R.C. and CHRISTIAN, J.L. Analysis of an Improved Boron/Aluminum Composite. ASTM STP 497, 1972, p. 439-468.

KOENIG, J.R. and FORNARO, G.F. Evaluation of the Compressive Properties of a Special 3DQP. AD-A044 031/3st, September 1976.

LAYNE, W.S. and PATRICK, R.L. Interfacial Interaction in Composite Structures. AD-665 697, November 1967.

LISIN, V.A. A Method of Detecting a Defective Layer in Double-Layer Articles Using the Radiometric Method of Electron Flaw Detection. Sov. J. of NDT, May 1979, p. 801-803.

LITTLETON, H.E. Collimated Scanning Radiography. SAMPE Journal, May-June 1978, p. 21-23

LOHSE, K.H. Application of Photographic Extraction Techniques to Nondestructive Testing of Graphites and Other Materials. AFML-TR-70-162, November 1970.

MAIGRET, J.P. and JUBE, G. Advanced NDT Methods for Filament Wound Pressure Vessels and Composites in General, Materials 1971, SAMPE 16th Nat. Symp. and Exhib., v. 16, April 1971, p. 123-137.

MANTEI, J.E. An Examination of Factors That Effect the Mechanical Properties of Boron-Aluminum Composites. AD-837 408/4st, June 1968.

MARCUS, L.A., STINCHCOMB, W.W. and TURGAY, H.M. Fatigue Crack Initiation in a Boron-Epoxy Plate With a Circular Hole. AD-780 106/1st, February 1974.

MATHERS, G.B. Nondestructive Inspection Techniques for Multilayer Circuit Boards. Mater. Eval., v. 25, no. 6, June 1967, p. 148-152.

MOOL, D.L. AND VANNIER, R.K. X-Ray Inspection of the AWACS Radome Attachment Locations. Mater. Eval., October 1972, p. 211-213.

MOORE, J.F. and MARTIN, G. Research and Development of Nondestructive Testing Techniques for Composites. AD-825 636/4st, AFML-TR-67-166, November 1967.

NEVADUNSKY, J.J., LUCAS, J.J., and SALKIND, M.J. Early Fatigue Damage Detection in Composite Materials. J. Compos. Mater., v. 9, October 1975, p. 394-408.

NEVADUNSKY, J.J., SALKIND, M.J. and LUCAS, J.J. Fatigue Damage Behavior in Composite Materials. AD/A-001 944/8st, September 1974

Nondestructive Testing Radiography. Defense Documentation Center, Alexandria, Virginia, AD-769 100/9, November 1973.

OWSTON, C.N. and JAFFE, E.H. Nondestructive Testing and Inspection Applied to Composite Materials and Structure. AD-739 789. February 1972.

PROUDFOOT, E.A. Nondestructive Testing Techniques for Advanced Composites. AD-714 296, September 1970.

REYNOLDS, W.N. Problems of Nondestructive Testing in Carbon Fibers and Their Composites. Int. Conf. Carbon Fibres and Their Comp., Appl. Pap., 1971, p. 52/1-52/5.

REYNOLDS, W.N. Testing of Fibre-Bonded Composites. SPI Reinf. Plas./Compos. Div., Proc. 24th Ann. Tech. Conf., Washington, Sect. 14E February 1969.
SALKIND, M.J. Early Detection of Fatigue Damage in Composite Materials. J. Aicr., v. 13, no. 10, October 1976, p. 764-769.
SCHULTZ, A.W. Development of Nondestructive Methods for the Quantitative Evaluation of Advanced Reinforced Plastic Composites. AD-875 229, 1970.
STONE, D.E.W. Nondestructive Inspection of Composite Materials for Aircraft Structural Applications. Brit. J. of NDT, March 1978, p. 65-75.
STONE, D.E.W. Some Problems in the Nondestructive Testing of Carbon Fiber-Reinforced Plastics. Carbon Fibres, 2nd Int. Conf.Proc., 18-20 February 1974, Paper 28, Plast. Inst., London, 1974.
STONE, D.E.W. The Use of Radiography in the Nondestructive Testing of Composite Materials. AD-894 884, December 1971.
WANG, A.S.D. and CROSSMAN, F.W. Initiation and Growth of Transverse Cracks and Edge Delamination in Composite Laminates, Part 1. -An Energy Method J. of Compos. Mater. Supplement, v. 14, 1980.
X-Ray Eye for Quality Control. British Plastics, v. 42, no. 9, September 1969.
ZURBRICK, J.R. Development of Nondestructive Methods for the Quantitative Evaluation of Glass-Reinforced Plastics. AFML-TR-66 269, March 1967.

Microradiography

BOOGEND, S.J., VAN ZUYLEN, P and FONTIJN, L.A. An Unconventional 150 Kv Microfocus X-Ray Equipment for NDT Purposes. November 1976, p. 175-178.
FONTIJN, L.A. and PEUGEOT, R.S. An Operational 150 Kv Microfocus Rod Anode X-Ray System for Nondestructive Testing NDT International, October 1978, p. 229-235.
GUGAN, K. A fine Focus High Intensity, Medium Energy X-Ray Source. J. Sci Instr., v 42, 1965.
HOTHAM, C.A., JONES, R.W. and TAYLOR, J.L. Microfocal Radiography Using the Electron Microscope. Brit. J. of NDT, November 1981, p. 306.
SMITH, R.L. The Effect of Scattering on Contrast in Microfocus Projection X-Radiography. Brit. J. of NDT, September 1980, p. 236-239.
WILLIAMS, R.D. General Applications of Microfocus X-Ray Techniques to the Field of NDT. 3rd Annual Symp. on NDT or Aircraft and Missile Components, 1962.

Automatic Computer Based Radiographic Image Enhancement

CLOSIER, M.J. Automatic Product Analysis Using X-Rays. NDT International, April 1981, p. 59-65.
GOSSELIN, R.M. Automatic Nondestructive Testing with X-Rays. Brit. J. of NDT, January 1973, p. 17-22.
HALL, E. L., et al A survey of Preprocessing and Feature Extraction Techniques for Radiographic Images. IEEE Trans. Computers C-20, no. 9, September 1971, p. 1032-1044.
HALMSHAW, R. and JAKINS, B.G. Optical and Digital Image Processing Applied to Radiographs. Brit. J. of NDT, July 1977, p. 197-199.
HARRINGTON, T.P., and DOCTOR, P.G. Data Analysis Methods for Nondestructive Evaluation. Battelle Pacific Northwest Labs, Report BN-SA-1056, October 1979.
HESSE, P.W., CRISCUOLO, E.L. and POLANSKY, D. Radiographic Image Enhancement by Spatial Frequency Filtering. Brit. J. of NDT, July 1973, p. 101-107.

HUNT, A.C. The effect of Masking in T.V. Image Intensifier Fluorscopy. Brit. J. of NDT, January 1981, p. 12-13.
HUNT, B.R. Digital Image Processing Proc. IEEE 63, no. 4, April 1978, p. 693-708.
PEARSON, J.J., FISCHLER, M.A., FIRSCHEIN, O. and JACOBY, M. Application of Image Processing Techniques to Automatic Radiographic Inspection. Proc. EIA 7th Annual AIPR Symposium, 1977.
SCHAGEN, P. X-Ray Imaging Tubes. NDT International, February 1981, p. 9-14.

Stereo Radiography

ADHIKARI, B.C., CHANDA, D.K. and JANA, S. On the Determination of the Depth of a Planar Defect by Radiography. Brit. J. of NDT, Tech. Note, September 1979, p. 249-251.
HALMSHAW, R. and HALSTEAD, F. Defect Size Measurement by Radiography. Brit. J. of NDT, September 1979, p. 245-248.

Opaque Additives

CHANG, F.H., GORDON, D.E. and GARDNER, A.H. A Study of Fatigue Damage in Composites by Nondestructive Testing Techniques. ASTM-STP 636, 1977, p. 57-72.
JENSEN, D.L. and SPENCE, L.M. Radiographic Enhancement Results and Structural Performance Effects of Diiodobutane on Graphite/Epoxy Structures. Lockheed Missiles and Space Company, Inc., Sunnyvale, California 94086.
KORNISHIN, K.I. Application of Contrasting Liquids in Roentenography. Industr. Laboratory, v. 30, no. 4, April 1964, p. 560-561.

Neutron Radiography

CARTER, A.C., MARTYN, N.P.W. and WILSON, C.G. Enhancement of Neutron Radiographic Contrast. Brit. J. of NDT, January 1980, p. 21-24.
HERMAN, H. Nondestructive Evaluation of Materials with Cold Neutron Beams. AD-A053 073, December 1973.
HOLLAND, B.G. Contrast Enhancement in Neutron Radiography Using a Gaseous Penetrant. Brit. J. of NDT, July 1980, p. 172-174.
HOLLOWAY, J.A. and STUHRKE, W.F. Low Voltage and Neutron Radiographic Techniques for Evaluating Boron Filament Metal Matrix Composites. AD-829 621/2st, February 1968.
JACKSON, C.M., BARTON, J.P. and PROUDFOOT, E.A. Neutron Radiography Facility at the Hanford Engineering Development Laboratory. Mater. Eval., June 1979, p. 55-61.
WILSON, C.R. Neutron Radiography Complements X-Rays. Metal Progress, v. 98 no. 2, August 1970, p. 75-76.

X-Ray Diffraction

BARRETT, C.S. and PREDECKI, P. Stress Measurement in Polymetric Materials by X-Ray Diffraction. Polym. Eng. and Sci., v. 16, no. 9, September 1976, p. 602-608.
BRYDGES, W.T., BADAMI, D.V., JOINER, J.C. and JONES, G.A. The Structure and Elastic Properties of Carbon Fibers. Appl. Polym. Symp. no. 9, 1969, p. 255-261.

PREDECKI, P. and BARRETT, C.S. Stress Measurement in Graphite/Epoxy Composites by X-Ray Diffraction from Fillers. J. Compos. Mater., v. 13, January 1979, p. 61-71.

SCHIERDING, R.G. Measurement of Whisker Orientation in Composites by X-Ray Diffraction. J. Compos. Mater., v. 2, no. 4, October 1978, p. 448-457.

SPERI, W.M. and JENKINS, C.F. Effect of Fiber-Matrix Adhesion on the Properties of Short Fiber Reinforced ABS. Polym. Eng. and Sci, v. 13, no. 6, November 1973, p. 409-414.

STANDARDIZATION DOCUMENT IMPROVEMENT PROPOSAL

(See Instructions – Reverse Side)

1. DOCUMENT NUMBER	2. DOCUMENT TITLE

3a. NAME OF SUBMITTING ORGANIZATION	4. TYPE OF ORGANIZATION *(Mark one)*
	☐ VENDOR
b. ADDRESS *(Street, City, State, ZIP Code)*	☐ USER
	☐ MANUFACTURER
	☐ OTHER *(Specify)*:

5. PROBLEM AREAS

a. Paragraph Number and Wording:

b. Recommended Wording:

c. Reason/Rationale for Recommendation:

6. REMARKS

7a. NAME OF SUBMITTER *(Last, First, MI)* – Optional	b. WORK TELEPHONE NUMBER *(Include Area Code)* – Optional
c. MAILING ADDRESS *(Street, City, State, ZIP Code)* – Optional	8. DATE OF SUBMISSION *(YYMMDD)*

(TO DETACH THIS FORM, CUT ALONG THIS LINE.)

DD FORM 82 MAR 1426

PREVIOUS EDITION IS OBSOLETE.